MDR1 deficiency impairs mitochondrial homeostasis and promotes intestinal inflammation

MDR1-deficiency impairs mitochondrial homeostasis and promotes intestinal inflammation

Gwo-Tzer Ho[1,2], Rhona E Aird[1,4], Bo Liu[3], Ray K Boyapati[1,2], Nicholas A Kennedy[2], David A Dorward[1], Colin L Noble[2], Takahiko Shimizu[5], Roderick N Carter[4], Etienne TS Chew[1], Nicholas M Morton[4], Adriano G Rossi[1], R. Balfour Sartor[3], John P Iredale[1,6], Jack Satsangi[2]

Corresponding author: Dr Gwo-Tzer Ho

[1]MRC Centre for Inflammation Research

Queens Medical Research Institute

University of Edinburgh

47 Little France Crescent

Edinburgh, EH16 4TJ, UK

Email: gho@ed.ac.uk

Tel No: 0131-242 6653

[2]Gastrointestinal Unit

Western General Hospital

University of Edinburgh

Edinburgh, EH4 2XU, UK

[3]Departments of Medicine, Microbiology and Immunology, Center for Gastrointestinal Biology and Disease

University of North Carolina

Chapel Hill, NC 27599-7032, USA

[4]University/BHF Centre for Cardiovascular Science

University of Edinburgh

47 Little France Crescent

Edinburgh, EH16 4TJ, UK

[5]Department of Advanced Aging Medicine,

University of Chiba

1-8-1 Inohana, Chuo-ku, Chiba 260-8670, Japan

[6]University of Bristol,

Bristol BS8 1TH, UK

Abstract

The multidrug-resistance-1 (*MDR1*) gene encodes an ATP-dependent efflux transporter that is highly expressed in the colon. In mice, loss of MDR1 function results in colitis with similarities to human inflammatory bowel diseases (IBD). Here, we show that MDR1 has an unexpected protective role for the mitochondria where MDR1-deficiency results in mitochondrial dysfunction with increased mitochondrial ROS (mROS) driving the development of colitis. Exogenous induction of mROS accelerates, whilst inhibition attenuates colitis *in vivo*; these effects are amplified in MDR1-deficiency. In human IBD, *MDR1* is negatively correlated to *SOD2* gene expression required for mROS detoxification. To provide direct evidential support, we deleted intestinal *SOD2* gene in mice and showed an increased susceptibility to colitis. We exploited the GWA datasets and found many (~5%) of IBD susceptibility genes with direct roles in regulating mitochondria homeostasis. As MDR1 primarily protects against xenotoxins via its efflux function, our findings implicate a distinct mitochondrial toxin + genetic susceptibility interaction leading to mitochondrial dysfunction, a novel pathogenic mechanism that could offer many new therapeutic opportunities for IBD.

Introduction

Inflammatory bowel diseases (IBD) are complex immune-mediated conditions that can be subclassified into the clinically distinct entities of Crohn's disease (CD) and ulcerative colitis (UC) [1,2]. Both are debilitating relapsing inflammatory conditions, which affect an estimated 4 million people in the United States and Europe with increasing prevalence in the developing world [3]. CD is characterised by discontinuous aphthous mucosal ulcerations and inflammation occurring most commonly in the distal small intestine (ileum) and variably across the intestinal tract[2].

UC affects only the large bowel (colon) in a confluent manner and is characterised by superficial mucosal inflammation[4]. Increasingly evident both in clinical and molecular studies is the concept that IBD involves multiple distinct and also, common pathogenic mechanisms. The powerful genomewide association (GWA) studies implicate more than 200 genetic susceptibility loci including genes in biological pathways regulating innate (e.g. *NOD2* and autophagy) and adaptive (e.g. *Th17, MHC*) immune responses, cytokine production, lymphocyte activation and bacterial response[5,6].

One major mechanistic theme that is shared between UC and CD is the role of intestinal epithelial dysfunction and injury[7]. The intestinal epithelium is uniquely in contact with high concentrations of bacteria with their metabolic products, immune-active ligands, damage-associated molecular products (DAMPs), xenobiotics and environmental toxins[8]. Thus, a central component of IBD pathogenesis is the de-regulation of protective mechanisms that maintain cellular homeostasis and resultant epithelial dysfunction. MDR1 is a key mediator of one such mechanism[9] by actively extruding more than 4000 diverse products, including xenotoxins, out of the intracellular environment[10]. MDR1 belongs to the ATP-binding cassette, ABC-transporter family of transmembrane transporters. These proteins bind ATP and use the energy to drive the transport of various molecules across all cell membranes. Genetic variations in this family of genes contribute to several human disorders including cystic fibrosis, neurological diseases, retinal degeneration, anaemia, cholesterol and bile transport defects[9].

Epithelial cells of the distal intestinal tract have very high MDR1 expression reflecting the importance of its cytoprotective role at the gut luminal interface [11]. In the mouse,

the *mdr1a* gene encodes PgP170. Constitutive genetic deletion of this gene results in chronic spontaneous colitis as the mutants age with ~50% penetrance when >6 months of age[12]. Interestingly, the *mdr1a*-deficient mice display no other spontaneous clinical phenotype, underlining the dominant physiologic role of *mdr1a* in the gut. Its importance in colonocytes is further highlighted by the lack of rescue from colitis when *mdr1a*-deficient mouse were reconstituted with *mdr1a*$^{+}$ bone marrow stem cells[12]. In human IBD, several studies have shown a downregulation of intestinal MDR1 expression[13,14]. *MDR1* has been linked to IBD in early human candidate genetic studies with disease-associated variants associated with low MDR1 expression[15]. These findings implicate the loss of MDR1 function as a contributory factor in the pathogenesis of IBD.

Although an underlying increase in intestinal permeability is considered as the dominant factor for the development of *mdr1a*-deficient colitis, the preceding steps leading to this late stage are not fully clarified[16]. In this study, we show for the first time that MDR1 confers a protective role to the gut epithelial mitochondria and that MDR1 deficiency results in mitochondrial dysfunction driving the development of colitis. The mitochondria play a key role in many physiologic processes such as energy production, regulation of cell death and immune response. Given that MDR1 is critically positioned at the interface between mitochondria and the luminal environment, this protective mechanism opens up a fresh perspective in how de-regulation of mitochondria homeostasis influences the development of colitis.

Results

Mdr1a-deficient colonic epithelium shows an accumulation of damaged mitochondria

Using transmission electron microscopy, we showed that the *mdr1a*-deficient mice displayed a preferential accumulation of damaged and degenerating mitochondria in colonic epithelial cells (CECs) in the inflamed colon (**Fig 1a**). CECs harbouring these mitochondrial abnormalities were found in higher frequencies in *mdr1a*-deficient mice compared to non-inflamed colon, ileum and liver in wild type (WT) mice (14% vs. <2% overall frequency) (**Figs 1b and S1a**). These features were not present in *il10*-deficient mice CECs, a spontaneous chronic colitis control group with a defined inflammatory mechanism[17] (**Fig S1b**) and only in necrotic CECs during acute dextran-sulphate sodium colitis (DSS). Immunohistochemistry analysis of *mdr1a*-deficient colons revealed increased colonic epithelial p62, PTEN-induced kinase 1 (PINK1) and superoxide dismutase-2 (SOD2) staining (**Fig 1c**). p62 is a ubiquitin-binding protein that promotes autophagic degradation of protein aggregates recognises damaged mitochondria and recruits them to the isolation membrane through its interaction with LC3[18]. PINK1 is involved in specific autophagic clearance of damaged mitochondria (or mitophagy) [19]; whereas SOD2 plays a role in detoxifying mitochondrial reactive oxygen species (ROS). Furthermore, isolated CECs confirmed higher p62, increased microtubule-associated protein 1 light chain 3-β, LC3-I to phosphatidylethanolamine (PE)-conjugated or LC3-II ratio indicative of heightened autophagy; and parkin expression in *mdr1a*-deficiency (**Fig S2a**). Parkin translocates to mitochondria upon dissipation of mitochondria membrane potential and cooperates with PINK1 during mitophagy. CEC voltage-dependent anion channel (VDAC) expression and mitochondria DNA were similar to WT, suggesting that these changes were not due to changes in mitochondria content (**Figs 1c and**

S2b). Mitochondria isolated from *mdr1a*-deficient CECs were more sensitive to mitochondrial membrane damage by *carbonyl cyanide m-chorophenyl hyrdrazone*, CCCP, a known damaging agent (**Fig 1d**). Furthermore, we detected increased circulating plasma mitochondrial DNA, a known inflammatory DAMP in *mdr1a*-deficient mice with colitis (**Fig 1e**). The *mdr1a*-deficient colons have increased epithelial cell turnover and death respectively (**Figs S2c, d**). MDR1-deficient mice exhibited clear evidence of colonic epithelial mitochondrial damage with increased epithelial dysfunction and cell-death.

MDR1 deficiency results in mitochondria dysfunction

To study the functional consequence of MDR1 deficiency on the mitochondria, we investigated the cellular energetics of primary colonic explants of *mdr1a*$^{-/-}$ and WT mice. We found lower basal O_2 consumption rate (OCR) in *mdr1a*$^{-/-}$ colon consistent with impaired mitochondrial function and energy production (**Figs 2a**). We further knocked down MDR1 expression *in vitro* by transducing short hairpin *MDR1* (*shMDR1*) in the human T84 CEC cell line (**Figs S3a**). Although we found no differences in OCR (**Figs S3b**), MDR1 deficiency in T84 CECs resulted in lower spare respiratory capacity (SRC) (**Fig 2b**). SRC is the extra mitochondrial capacity available in a cell to produce energy under conditions of increased work and stress and is thought to be important for long-term cell survival and function [20]. Dysfunctional or damaged mitochondria produce increased levels of ROS and the mitochondria are the major source of ROS for most cells[21]. In line with our observations in *mdr1a*-deficient mouse CECs, we found increased levels of mROS in *shMDR1* T84 CECs at baseline (**Fig 2c**); and following artificial induction with rotenone and antimycin by fluorescence of MitoSOX (a mitochondrial superoxide indicator) (**Fig 2d**). Furthermore, we showed that *MDR1*-knockdown resulted in

higher p62 and SOD2 protein expressions following rotenone treatment in *shMDR1* CECs (**Fig S3c**). We transfected LC3-GFP and found reduced autophagy (**Fig 2e**); and LC3-II protein after inhibition of its degradation by bafilomycin (**Fig S3d**) in *shMDR1* relative to *shCtrl* CECs. This suggests a depressed clearance that compounds mitochondria dysfunction. Degenerating mitochondria in CECs are notably present in mice models with primary autophagy (*Irgm* and *Atg16l1*)[22,23], secondary autophagy impairments due to defective ER-stress [24] and NLRP6 inflammasome activity [25]. Our data collectively show that loss of MDR1 results in mitochondria dysfunction with impaired bioenergetics, increased mROS production and perturbed autophagic clearance.

Experimental induction of colonic mitochondria ROS influences the development of colitis in MDR1a-deficiency

We then sought to investigate if induction of mROS can accelerate the development of colitis in *mdr1a*-deficiency. We developed an *in vivo* protocol to test this further by directly administrating rotenone with low dose DSS (0.25%) into the colon of *mdr1a*-deficient and WT mice. We chose rotenone to specifically focus on the effects of mROS and to test its early effects prior to full induction of DSS colitis. Rotenone is primarily an inhibitor of mitochondrial complex I of electron transport chain which results in increase mROS production and at higher doses, cellular bioenergetic deficit[26]. Rotenone is a well-described triggering factor for rodent models of Parkinson's disease and is administered systemically (by injection) and/or orally[27]. Given that direct colonic administration *in vivo* is a new approach, we titrated the colonic rotenone concentration to 100μM (equating to ~1mg/kg) without systemic ill effects, notably respiratory, neurological and motor deficits (**Fig S4a**)**.** Drug dosing data derived from rodent rotenone-induced Parkinson's disease ranged between 2.5-

15mg/kg systemically to 0.25-100mg/kg orally[26] with increased mortality is observed in the former approach. Within 24 hours of 100μM rotenone administration, we found that this is sufficient to trigger increased leukocyte infiltration and colitis in *mdr1a*-deficient mice, which are not present in WT mice (**Figs S4b, c**) associated with increased CEC death in *mdr1a*-deficient colon (**Figs S4d, e**). We expanded our protocol where we directly administered 500μl of 100μM of rotenone 3 times/week over 4 weeks in the absence of DSS (**Fig 3a**). In *mdr1a*-deficient mice with no prior evidence of colitis, we found that this accelerated the onset of colitis compared to vehicle (**Fig 3b, c**). In *mdr1a*-deficiency, rotenone-treated mice have more severe colitis compared to the vehicle group (**Fig 3d-f**). Isolated CECs from rotenone-treated *mdr1a*-deficient mice have higher pro-inflammatory *il6* and *tnf-α* gene expressions (**Fig S4f**). In addition to triggering spontaneous colitis, exogenous induction of mucosal mROS using rectal rotenone treatment (**Fig 3g**) rendered the *mdr1a*-deficient mice more susceptible to acute DSS colitis exhibiting more severe clinical and histologic evidence of inflammation (**Fig 3h-j**). To investigate the effects of rotenone on the epithelial barrier, we further showed that *shMDR1* compared to *shCtrl* CECs have an increased sensitivity to rotenone, CCCP and cisplatin-induced cell death (**Figs S5a, b**) and displayed an increased loss of barrier function as measured by transepithelial electric resistance following culture with rotenone (**Fig S5c**). In line with our *in vivo* data, we also showed that mROS-induced by rotenone triggered increased colonic epithelial IL-8 production induced by flagellin and bacterial CpG (these ligands chosen as our T84 CECs express *TLR5* and *TLR9*) (**Fig S6d**), indicating that mROS triggers CEC-death and innate inflammatory responses. Collectively, these data suggest that abnormal mucosal mROS driven by an exogenous trigger can influence the onset and severity of colitis in a genetically susceptible host, in this respect, MDR1-deficiency.

Inhibition of mitochondria ROS effects attenuates and promotes recovery from colitis *in vivo*

Next we investigated whether inhibiting the effects of mROS can prevent or attenuate the development of colitis. Mitoquinone (MitoQ) is a mitochondrial specific antioxidant with coenzymeQ_{10} covalently attached to a triphenylphosphonium molecule, which selectively accumulates within the mitochondria. MitoQ protects the mitochondria membrane from mROS-induced lipid peroxidation and acts as a ROS-scavenger[28]. We first investigated the effect of mROS inhibition in *mdr1a*-deficient chronic colitis. Here, we tested the effects of colonic MitoQ (10μM), rotenone and vehicle only in *mdr1a*-deficient mice with clinical evidence of chronic colitis (10-12 weeks old, all with chronic diarrhoea) (**Fig 4a**). Colonic MitoQ improved colitis in *mdr1a*-deficient mice (**Figs 4b-d, S6a**). In contrast to earlier data from *mdr1a*-deficient mice with no colitis, rotenone surprisingly, did not further exacerbate chronic colitis. We think this may be due to the intrinsic nature of *mdr1a*-deficient colitis model where the main driving factor is increased barrier permeability. Hence, colonic mitochondrial dysfunction in this setting acted as a triggering factor and once barrier function was compromised resulting in colitis, rotenone has a lesser role to worsen colitis in this model. Here, the histologic severity scores in both rotenone and control groups were 8 and 9.5 respectively out of the maximal score 12. The high baseline made it difficult to test for an exacerbating role for rotenone. In acute DSS-colitis, colonic MitoQ delayed the onset in *mdr1a*-deficient mice (**Fig 4f**) and significantly attenuated colitis in WT mice (**Figs 4g, S6b**). In both settings, there were histologic improvements in the severity of colitis (**Fig 4h**). We also showed that MitoQ improved clinical recovery following 5 days of DSS challenge (**Figs 4i, S6c**). In this setting, we tested only WT mice, as *mdr1a*-deficient mice were too unwell after DSS-induction. Two recent

studies corroborate the protective effects of MitoQ in acute DSS colitis (although via oral route) [29,30]. Inhibiting the effects of mROS is therefore beneficial in acute and chronic colitis as well as during the recovering phase of colitis.

MDR1 and _SOD2_ genes are differentially expressed in human IBD and intestinal epithelial specific deletion of _SOD2_ leads to increased susceptibility to experimental colitis

To further investigate the role of MDR1 and mROS in human IBD, we performed an *in silico* analysis of our IBD colonic microarray dataset (Gene Expression Omnibus GSE11223 and GSE20881) derived from a cohort of 67 individuals with UC, 53 with CD, 14 non-IBD colitis and 31 healthy controls[13,31]. Colonic gene microarray expression data were available from 118 inflamed IBD, 110 non-inflamed IBD and 50 healthy non-IBD colonic biopsies. In addition to significant downregulation of *MDR1* expression in inflamed vs. non-inflamed IBD intestinal biopsies and inflamed IBD vs. healthy non-IBD intestinal biopsies ($p<0.0001$ and 0.0003 respectively); we interestingly found differential expression of *SOD2* expression (upregulated) in both analyses ($p<0.001$ and 0.0002) (**Fig 5a, b**). *MDR1* negatively correlated with *SOD2* ($r= -0.47$, $p<0.0001$) in line with our earlier findings in *mdr1a*-deficient mice and *shMDR1* CECs (**Fig 5c**). It is essential to determine whether primary ROS-mediated mitochondria dysfunction acts causally to promote the development of colitis. Furthermore, there may be factors such as variability in tissue penetration and retention that cannot be completely accounted for in the colonic rotenone exposure model. Therefore we genetically deleted the *SOD2* gene from the intestinal epithelium by crossing $SOD2^{floxed/floxed}$ mice with mice expressing *Cre-recombinase* under the control of the intestinal-epithelial-specific villin promoter to $SOD2^{IEC\text{-}KO}$ mice (**Fig 5d**). Constitutive deletion of *SOD2* gene in mice resulted in death early after

birth from cardiac and liver failure[32]. In our study, *SOD2*$^{IEC\text{-}KO}$ mice were born in normal Mendelian ratio and had no overall abnormalities in the morphology of ileum and colon. Although they did not exhibit spontaneous colitis, *SOD2*$^{IEC\text{-}KO}$ developed more severe colitis following DSS treatment compared to *SOD2*$^{floxed/floxed}$ littermates (**Fig 5e-g**). Our data in *SOD2*$^{IEC\text{-}KO}$ mice provides evidential support for the loss of mitochondrial homeostasis in CECs as a specific factor in determining susceptibility to colitis.

Associations of genes regulating mitochondrial function with human IBD

Finally, to demonstrate clinical relevance of mitochondrial dysfunction as a new mechanistic factor in IBD, we exploited data from the latest meta-analysis of GWA studies of all European ancestry IBD patients vs. European controls (22,575 CD, 20,417 UC and 53,536 controls) [6]. The most significant loci in the regions of *ABCB1* (encoding MDR1) and *SOD2* genes showed associations with $p=3.19 \times 10^{-3}$ and 3.04×10^{-3} respectively (below genome-wide significance). We performed an independent unbiased analysis (using GO term for mitochondria, GO:0005739 using the Mitominer program http://mitominer.mrc-mbu.cam.ac.uk/release-3.1) and identified 29 (5.0%) additional genes involved in mitochondria function within the subset of 574 (out of total 22 353) genes within 100kb of a genome-wide significant IBD locus from the same meta-analysis dataset above (**Table S1**). The top three positional candidate gene associations are: *SLC25A28* ($p=1.70 \times 10^{-26}$) encoding mitoferrin-2, *VARS* encoding valine-tRNA ligase ($p=4.83 \times 10^{-26}$) and *RNF5* ($p=9.47 \times 10^{-24}$) encoding E3 ubiquitin-protein ligase RNF5 are involved in mitochondria iron, tRNA transport and ubiquitination respectively[33-35]. Notable also, are the associations of the *HSPA1-A, -B* and *–L* ($p=1.88 \times 10^{-23}$) genes that encode the heat shock protein 70, which is integrally involved in the mitochondria unfolded protein responses (mtUPR),

crucial for mitochondria protein homeostasis and biogenesis[36]. This suggests that the mitochondria's contribution is likely more important than previously recognised in IBD.

Discussion

In this study, we define a key mitochondrial protective mechanism conferred by MDR1. Here, we present clear evidence of increased mitochondrial damage and consequential dysfunction following MDR1-deficiency with increased susceptibility to colitis driven by mitochondrial dysfunction *in vivo*. We therefore highlight a cogent model to further support mitochondrial dysfunction as an important mechanistic component in the pathogenesis of IBD (reviewed by Novak and Mollen) [37]. We show conceptually that at the dynamic colonic mucosal interface in particular, mitochondria homeostasis requires tight regulation to prevent the deleterious downstream effects on epithelial integrity, activation of pro-inflammatory responses and release of mitochondria DAMPs as *bona fide* inflammatory triggers. The mitochondria participate in a broad range of innate responses to viral, bacterial and cellular damage[38]. Recently mitochondria have an increasingly recognized role in inflammation[38] and are implicated in human diseases with underlying inflammatory pathologies, such as diabetes[39], multiple sclerosis[40], lung fibrosis[41] and cardiovascular disease[42].

Our data suggest an intricately linked picture, where MDR1 protects against damaging mitochondrial factors arising from the luminal environment via its efflux properties in addition to exerting an influence on key homeostatic responses such as energy production and autophagy. The compositional factors within the lumen in this context; and alternatively, mechanisms that affect the functionality of MDR1 have not

yet been studied in detail. As an ATP-dependent efflux transporter, gut energy deficiency is a likely important factor. In the colon, mitochondria rely on the gut microbiota and their production of short chain fatty acid for energy [43] and CEC energy deficiency has been previously purported to be an IBD mechanism. Mouse lines with mitochondria genomic variants linked to high ATP production are protected against induced colitis [44]. Whilst analysis of cellular bioenergetics in primary explants showed impairment in energy production, our *in vitro* CEC data indicate a more modest effect without the contribution of the luminal flora, with decreased CEC spare respiratory capacity in the presence of diminished MDR1 activity. The lack of baseline OCR differences *ex vivo* and *in vitro* may reflect fundamental differences in genetic knock-down rather than knock-out, inherent bioenergetic properties of colonic 'cancer' cell line and *in vitro* conditions that provided a more stable environment for mitochondrial function. In mouse, colonisation of specific gut commensals can influence the level of MDR1 gene expression[45]. Hence, it is conceivable that a primary effect of MDR1-deficiency on mitochondrial bioenergetics is potentiated by factors present in the luminal environment in the colon, chiefly the microbiota. In IBD, high levels of mitochondria damage, notably within the electron transport chain have been shown in CECs [46] and the resident luminal microbiota are strongly implicated in the pathogenesis of IBD[8].

The evidence to support directly harmful effect of the microbiota on the mitochondria is noteworthy. Individuals with IBD have higher levels of anaerobic sulphate reducing bacteria, which can produce metabolites that can damage the mitochondria, inhibit cytochrome C and short chain fatty acid oxidation[47]. Within the gut flora, several clinically relevant pathogens including enteropathogenic *E. coli* [48] *Helicobacter pylori* [49] and *Salmonella typhimurium* [50] target effector proteins to the mitochondria.

Infection with *Citrobacter rodentium* has been shown to disrupt mitochondrial function and structure in mice [51]. These lines of evidence suggest that the gut mitochondria occupy a distinct position as they are more exposed to damaging luminal factors, more so than in other tissues. Hence, it follows that different protective mechanisms are shaped to counter this challenge. In a proteomic analysis across 14 different mouse tissues, Pagliarini *et al.*, demonstrated that intestinal epithelial mitochondria have a distinct proteomic profile and notably, have higher expression of ABC transporters [52]. MDR1 (although part of the ABC superfamily) is not expressed on the mitochondria membrane[53] but the closely analogous functions of these transporters highlight the importance of this protective role for the mitochondria in the gut.

Beyond the microbiota, the role of luminal mitochondrial toxins as triggers in IBD is unknown but seems plausible. Findings from Parkinson's disease (PD), a condition characterized by marked mitophagy impairment [54,55] provides insight into how this might work in IBD pathogenesis. Here an environmental mitochondrial toxin, *N-methyl-4-phenyl-1,2,3,6-tetrahydropyridine* (MPTP) represents a clear trigger for clinical PD. Like rotenone, MPTP is a complex I inhibitor of the electron transport chain that can induce acute PD that is indistinguishable from idiopathic PD[56-58]. Current literature suggests that rotenone may possess potential effects on the direct aggregation of protein aggregates such as α-synuclein (SNCA), ubiquitin and GAPDH; alterations of dopamine metabolism; and microglial activation via NFKB activation[26]. There maybe off-target actions too but given its dominant effect on mitochondria respiratory function, these may be difficult to detect. Even though the role for autophagy in general is clearly established in IBD, mitophagy has not yet been fully studied in this context [5,59]. Strikingly and on further analysis however, genes involved in mitophagy (*PARK7 chr1p36*; $p=4.8x10^{-9}$ for UC; and *LRRK2*

chr12q12; p=6.2x10^{-21} for CD) are strongly associated with IBD in GWA studies. In parallel, defective mitophagy has been demonstrated in colonic epithelial cells derived from *Irgm1*-deficient mice, implicating this pathway in another IBD- associate gene polymorphism[23]. Like the virus-plus-susceptibility gene interaction that determines CD susceptibility as proposed by Cadwell *et al.* in 2010, we put forward the concept of mitochondrial toxin-plus-genetic susceptibility[60]. In this regard, we show that rotenone can accelerate the development of spontaneous colitis in the susceptible *mdr1a*-deficient model and in acute-induced DSS colitis, a setting when a second 'hit' along with rotenone exacerbates the severity of colitis. We believe that this is the first description of such kind although the protective effects of mitochondrial specific anti-oxidant (MitoQ) and more generally, anti-oxidants such as ascorbic acid have been described in experimental colitis[29,30 61].

Mitochondrial dysfunction via ROS production is a major mediator of inflammation and can directly modulate the NLRP3 inflammasome, NFKB and MAPK signalling pathways[62,63]. Mitochondrial ROS also promote the cytosolic release of mtDNA, which mediates NLRP3 inflammasome activation and can directly trigger TLR9 signalling on neutrophils[64-66]. Accumulation of dysfunctional mitochondria perpetuate the production of mROS, amplifying innate inflammatory responses such as type I interferon[67] and endotoxin induced IL-1β production[68]. Mitochondrial ROS inhibits autophagy, the major process for removal of damaged mitochondria[64]. Defective autophagy in turn allows for the escape of pro-inflammatory mitochondrial DAMPs [66] [65]. Our published colonic microarray study showing that gene-sets regulating the mitochondria (p=4.7×10^{-25}) and oxido-reductase functions (p=1.4×10^{-13}) were most differentially expressed comparing distal (where UC invariably affects) vs. proximal colon in UC. Further *in silico* analyses showed a negative correlation between *MDR1*

and *SOD2*, and our data showing increased susceptibility to DSS colitis following intestinal epithelial specific deletion of the SOD2 gene strongly supports the causal importance of ROS-detoxification.

IBD pathogenesis is complex and encompasses multiple factors, which may trigger disease onset, heighten susceptibility, potentiate severity and/or promulgate non-resolution of inflammation. These factors combine to shape the many phenotypes of IBD. In this context, our data importantly highlight the mitochondria's contribution as a new 'jigsaw' piece, a hitherto underexplored focus within this complex framework of factors. Specific pharmacologic MDR1 augmentation is a translational challenge due to induction of drug resistance as one known problem. However, our studies open up a new landscape of potential therapeutic approaches targeting downstream effects of mROS-DAMP, cellular bioenergetics and mitophagy as clear examples. Furthermore, we show that 5% of genes highlighted by IBD GWA studies are functionally linked to the maintenance of mitochondria health. Hence, the focus on mitochondrial dysfunction has broad translational applications, which will lead to many new mechanistic perspectives and therapeutic opportunities in IBD.

Materials and Methods

Mouse

The FVB/129 *mdr1a*$^{-/-}$ and wild type mouse lines were purchased from Taconic. C57/BL6 mice carrying floxed allele flanking *SOD2* gene was provided by Dr Shimizu, Chiba University, Japan and re-derived in University of Edinburgh. Villin-Cre recombinase C57/BL6 mice were purchased from Jackson laboratory. All colonies were maintained in specific pathogen free conditions (specifically Helicobacter-free)

in University of Edinburgh. *Il10*-deficient mice were maintained at University of North Carolina, Chapel Hill.

Electron microscopy

Mouse or human colonic samples were flushed with sterile phosphate buffered saline (PBS) and immediately transferred into 3% EM grade glutaraldehyde solution in 0.1M Sodium Cacodylate buffer, pH 7.3, for 2 hours before further processing. For quantification of abnormal mitochondria, viable cells with 5 or more abnormal mitochondria were classified as 'abnormal'. A percentage against total number of IECs (minimum of 100 IECs in >5 images) was calculated per mouse.

Mitochondria studies

Mitochondria from CECs or mouse tissues were performed using Dounce homogenisers (30-40 strokes in 2 different gradients of homogenisers) extracted using Mitochondria Isolation Kit (Sigma-Aldrich, MITOISO1). For JC-1 assay, the mitochondria pellets were re-suspended in 100µl storage buffer + 1900µl JC-1 assay buffer + JC-1. Mitochondria suspensions were placed in clear-bottom black 96 wells plate: untreated, Antimycin 10µg/ml, rotenone 10µM and CCCP 10µM. JC-1 fluorescence was measured using the plate reader at 590nM. The rate of mitochondria membrane depolarisation was measured as the loss of JC-1 fluorescence after 1 hour. Measurements were normalised to the untreated group. For mROS studies, T84 CECs were plated and grown in 96 well tissue culture plates for at least 24-48 hours and to ~70% confluence. Cells were cultured in MitoSOX (2.5µM) or mitotracker Green (100nM) for 30 minutes and then washed in pre-warmed PBS before further culture with Antimycin (20µg/ml), rotenone (10µM) or CCCP (10µM). Relative fluorescence (RF) was quantified using the plate reader at

Ex/Em 510/580 and 490/516 for MitoSOX and Mitotracker Green respectively. MitoSOX/MitoGreen RF readings were normalised to untreated MitoSOX/Mitotracker Green cells only.

Cellular energetics studies

Colon and ileum were harvested and placed in DMEM/F12 medium. A 3x3mm intestinal section was cut and mounted in Seahorse XF24 culture plate with the apical side of the lumen orientated upwards and maintained in position by an Islet Microcapture screen. The explants were washed twice with Seahorse Assay Media, supplemented with 1mM Pyruvate and 10mM Glucose (pH 7.4 at 37°C). These explants were placed into Seahorse analyzer within 1 hour of tissue harvest. We measured oxygen consumption rate (OCR) following addition antimycin/rotenone; providing mitochondrial function. The raw data were normalised to protein content using the Bradford quantification. T84 *shMDR1* and *shCtrl* CECs were plated on Seahorse XF 24 cell culture plates. For the mitochondria stress test oligomycin was added added at 2μM, followed by 1μM FCCP then antimycin and rotenone (1μM each). Data was normalised to protein content measured by sulforhodamine B staining (Sigma S1402) to adjust for cell density.

Induction and histologic grading of colitis

Colonic rotenone or vehicle were administered using a flexible rectal tube following brief general anaesthesia with isofluorane. A volume of 500μl were used in a head-down position for at least 2 minutes before removal of anaesthesia and then immediately check for any complications. The rotenone concentration of 100μM (volume of 500μl) equates to approximately 1mg/kg. In prior optimisation, we have

tested that this volume completely filled the mouse colon to provide total exposure. Acute colitis was induced by 2-3% DSS (MP Biomedicals Ltd) in drinking water *ad libitum* for 7-10 days. Mice were monitored daily for weights, presence of diarrhoea and blood. In chronic rotenone treatment, mice were assessed at the end of every week. Specifically, we quantified stool consistency: Well-formed/normal = 0, Pasty/semi-formed = 1, Pasty = 2, Diarrhoea that does not adhere to anus = 3, Diarrhoea that adheres to anus = 4. For histology, each colonic sample was graded semi-quantitatively (Scores 0-3 per component): A. Degree of epithelial hyperplasia and goblet cell depletion. B. Leukocyte infiltration in the lamina propria. C. Area of tissue affected. D. Presence of markers of severe inflammation (such as crypt abscesses, submucosal inflammation and presence of ulcers). For colitis scores, the mean of proximal and distal colon scores was calculated.

Quantification of mitochondrial DNA

Plasma samples were obtained by cardiac puncture following CO_2 euthanasia. Following sampling, blood samples were spun at 5 000x G for 10 minutes at 4C. DNA was extracted using Qiagen DNA Blood mini kit. Primer sequences for Cytochrome C oxidase sub-unit I (mCOI, Forward 5-GCCCCAGATATAG-CATTCCC-3; Reverse, 5-GTTCATCCTGTTCCTGCTCC-3) with qPCR performed using 2x SYBR Green Fast mix (Applied Biosystems). qPCR reactions were conducted in an ABI7900 Fast Real-Time PCR System (Applied Biosystems) with the following thermal profile: 1 cycle 95C for 20 sec; 40 cycles of 95C for 3 sec and 60C for 30 sec. mtDNA levels were quantified based on the following calculation: $c = Q \times V_{DNA}/V_{PCR} \times 1/V_{ext;}$ where c is the concentration of DNA in plasma (copies/µl); Q is the quantity (number of copies) of DNA determined by the qPCR system; V_{DNA} is the total volume of eluted plasma DNA solution obtained after extraction (40µl); V_{PCR} is

the volume of plasma DNA used for PCR (40µl); and V_{ext} is the volume of plasma extracted (200µl). Quantification was achieved relative to a known concentration of PCR amplicon obtained from DNA extracted from mouse CEC mitochondria using method previously reported.

Microarray dataset and analysis

Full detail of tissue acquisition and process are previously detailed [13]. The whole data set is available at Gene Expression Omnibus (http://www.ncbi.nlm.nih.gov/geo/ (accessed 18 July 2008)[6]) accession: GSE11223 and GSE20881.

Genetic analyses

The presented data was derived from the meta-analysis of all European ancestry IBD patients vs. European controls [6]. Analysis was done in R 3.2.2 (R Foundation for Statistical Computing, Vienna, Austria) using the Genomic Ranges package[33]. The UCSC hg19 Known Gene transcripts were filtered to keep only those with an associated Entrez Gene ID. For each Gene ID the earliest start and latest end position was taken from all of the transcripts for that gene. All p values within 100kb of each range were then associated with the respective Gene ID.

shRNA knockdown studies and transfection

T84 cells (purchased from ATCC) cells expressing MDR1 were transfected with MDR1 and control shRNA plasmids (SABiosciences) and selected using G418 (600ug/ml). Cells were cultured in DMEM/F12medium with 10% foetal calf serum, 100U/ml penicillin and 100ug/ml streptomycin. GFP-LC3 plasmid was transfected by Lipofectamine method (1:2 ratio) with GFP-plasmid controls to confirm transfection efficiency. Transfection was carried out on *shMDR1* and *shCtrl* CECs grown on glass

coverslips, which were then fixed with 4% paraformaldehyde and then viewed under fluorescence microscope.

Colonic epithelial cell isolation

Colons were removed and immediately placed in cold sterile PBS. Colons were opened longitudinally and further washed with buffer (154mM NaCl + 1mM dithiothreitol, DTT) three times. These were then placed in 5mL dissociation buffer (130mM NaCl, 1mM Na_2EDTA, 10mM HEPES, 10% FCS, 1mM DTT) in a bijou and placed on a shaker at 140rpm at 37^{o}C for 15 mins. Dissociated cells were placed in 15mL Falcon tube on ice. Incubation in dissociation buffer was repeated with another 2 x 5mL. Dissociated cells were spun at 2,500rpm for 10min at 4°C. Pellet was washed with PBS, spun at 5000rpm for 5min at 4°C.

Authors' contributions

GTH planned and carried out experiments, analysed data and wrote the manuscript. REA performed the *in vitro* cell line work, transfection studies and gene/protein expression studies. RNC, ETSC, REA and NM planned, carried out and analysed the mitochondria Seahorse experiments. BL planned and assisted in mouse colitis studies, performed histologic analysis and TEM work. DAD set up the mitochondria DNA qPCR work and performed data analysis. NAK recruited IBD subjects and prepared plasma samples for human mitochondrial DNA work, and performed additional *in silico* microarray and genetic analyses. CLN carried out original work of human IBD microarray work. TS generated SOD2 mouse mutants. RBS provided C57/BL6 transgenic strains (*mdr1a*$^{-/-}$ and *il10*$^{-/-}$). RBS, AGR, JPI and JS provided intellectual input into planning of experiments, data analysis and contributed to the writing of the manuscript. All authors reviewed and approved the final manuscript.

Acknowledgements

This work was supported by MRC grant G0701898, Crohn's and Colitis UK M16-1, ECCO IBD Investigator's Award 2010, Chief Scientist Office ETM/75 awarded to GTH; NIH grants P01 DK 094779 and R01 DK053347 awarded to RBS; Wellcome Trust Investigator Award WT100981MA to NMM; Wellcome Trust grant WT096497 to DAD and AGR; Wellcome Trust WT097943 to NAK; Wellcome Trust Biomedical Vacation Scholarship 202597/Z/16/Z to ETSC; EU FP-7 grants 305676-2 and 305479-2 to JS.

References

1. Danese, S. & Fiocchi, C. Ulcerative colitis. *The New England journal of medicine* **365**, 1713-1725 (2011).
2. Boyapati, R., Satsangi, J. & Ho, G.T. Pathogenesis of Crohn's disease. *F1000prime reports* **7**, 44 (2015).
3. Molodecky, N.A.*, et al.* Increasing incidence and prevalence of the inflammatory bowel diseases with time, based on systematic review. *Gastroenterology* **142**, 46-54.e42; quiz e30 (2012).
4. Ho, G.-T., Boyapati, R. & Satsangi, J. Ulcerative colitis. *Medicine* **43**, 276-281 (2015).
5. Jostins, L.*, et al.* Host-microbe interactions have shaped the genetic architecture of inflammatory bowel disease. *Nature* **491**, 119-124 (2012).
6. Liu, J.Z.*, et al.* Association analyses identify 38 susceptibility loci for inflammatory bowel disease and highlight shared genetic risk across populations. *Nature genetics* **47**, 979-986 (2015).
7. McCole, D.F. IBD candidate genes and intestinal barrier regulation. *Inflammatory bowel diseases* **20**, 1829-1849 (2014).
8. Sartor, R.B. & Wu, G.D. Roles for Intestinal Bacteria, Viruses, and Fungi in Pathogenesis of Inflammatory Bowel Diseases and Therapeutic Approaches. *Gastroenterology* (2016).
9. Dean, M., Rzhetsky, A. & Allikmets, R. The human ATP-binding cassette (ABC) transporter superfamily. *Genome research* **11**, 1156-1166 (2001).
10. Ambudkar, S.V.*, et al.* Biochemical, cellular, and pharmacological aspects of the multidrug transporter. *Annual review of pharmacology and toxicology* **39**, 361-398 (1999).
11. Thiebaut, F.*, et al.* Cellular localization of the multidrug-resistance gene product P-glycoprotein in normal human tissues. *Proceedings of the National Academy of Sciences of the United States of America* **84**, 7735-7738 (1987).
12. Panwala, C.M., Jones, J.C. & Viney, J.L. A novel model of inflammatory bowel disease: mice deficient for the multiple drug resistance gene, mdr1a, spontaneously develop colitis. *Journal of immunology (Baltimore, Md. : 1950)* **161**, 5733-5744 (1998).
13. Noble, C.L.*, et al.* Regional variation in gene expression in the healthy colon is dysregulated in ulcerative colitis. *Gut* **57**, 1398-1405 (2008).
14. Langmann, T.*, et al.* Loss of detoxification in inflammatory bowel disease: dysregulation of pregnane X receptor target genes. *Gastroenterology* **127**, 26-40 (2004).
15. Onnie, C.M.*, et al.* Associations of allelic variants of the multidrug resistance gene (ABCB1 or MDR1) and inflammatory bowel disease and their effects on disease behavior: a case-control and meta-analysis study. *Inflammatory bowel diseases* **12**, 263-271 (2006).
16. Resta-Lenert, S., Smitham, J. & Barrett, K.E. Epithelial dysfunction associated with the development of colitis in conventionally housed mdr1a-/- mice. *American journal of physiology. Gastrointestinal and liver physiology* **289**, G153-162 (2005).
17. Kim, S.C.*, et al.* Variable phenotypes of enterocolitis in interleukin 10-deficient mice monoassociated with two different commensal bacteria. *Gastroenterology* **128**, 891-906 (2005).
18. Pankiv, S.*, et al.* p62/SQSTM1 binds directly to Atg8/LC3 to facilitate degradation of ubiquitinated protein aggregates by autophagy. *The Journal of biological chemistry* **282**, 24131-24145 (2007).
19. Youle, R.J. & Narendra, D.P. Mechanisms of mitophagy. *Nature reviews. Molecular cell biology* **12**, 9-14 (2011).
20. Choi, S.W., Gerencser, A.A. & Nicholls, D.G. Bioenergetic analysis of isolated cerebrocortical nerve terminals on a microgram scale: spare respiratory capacity and stochastic mitochondrial failure. *Journal of neurochemistry* **109**, 1179-1191 (2009).
21. Brookes, P.S., Yoon, Y., Robotham, J.L., Anders, M.W. & Sheu, S.S. Calcium, ATP, and ROS: a mitochondrial love-hate triangle. *American journal of physiology. Cell physiology* **287**, C817-833 (2004).
22. Adolph, T.E.*, et al.* Paneth cells as a site of origin for intestinal inflammation. *Nature* **503**, 272-276 (2013).
23. Liu, B.*, et al.* Irgm1-deficient mice exhibit Paneth cell abnormalities and increased susceptibility to acute intestinal inflammation. *American journal of physiology. Gastrointestinal and liver physiology* **305**, G573-584 (2013).

24. Kaser, A.*, et al.* XBP1 links ER stress to intestinal inflammation and confers genetic risk for human inflammatory bowel disease. *Cell* **134**, 743-756 (2008).
25. Elinav, E.*, et al.* NLRP6 inflammasome regulates colonic microbial ecology and risk for colitis. *Cell* **145**, 745-757 (2011).
26. Xiong, N.*, et al.* Mitochondrial complex I inhibitor rotenone-induced toxicity and its potential mechanisms in Parkinson's disease models. *Crit Rev Toxicol* **42**, 613-632 (2012).
27. Johnson, M.E. & Bobrovskaya, L. An update on the rotenone models of Parkinson's disease: their ability to reproduce the features of clinical disease and model gene-environment interactions. *Neurotoxicology* **46**, 101-116 (2015).
28. Murphy, M.P. & Smith, R.A. Targeting antioxidants to mitochondria by conjugation to lipophilic cations. *Annual review of pharmacology and toxicology* **47**, 629-656 (2007).
29. Wang, A.*, et al.* Targeting mitochondria-derived reactive oxygen species to reduce epithelial barrier dysfunction and colitis. *The American journal of pathology* **184**, 2516-2527 (2014).
30. Dashdorj, A.*, et al.* Mitochondria-targeted antioxidant MitoQ ameliorates experimental mouse colitis by suppressing NLRP3 inflammasome-mediated inflammatory cytokines. *BMC medicine* **11**, 178 (2013).
31. Noble, C.L.*, et al.* Characterization of intestinal gene expression profiles in Crohn's disease by genome-wide microarray analysis. *Inflammatory bowel diseases* **16**, 1717-1728 (2010).
32. Li, Y.*, et al.* Dilated cardiomyopathy and neonatal lethality in mutant mice lacking manganese superoxide dismutase. *Nature genetics* **11**, 376-381 (1995).
33. Lawrence, M.*, et al.* Software for computing and annotating genomic ranges. *PLoS Comput Biol* **9**, e1003118 (2013).
34. Zhong, B.*, et al.* The ubiquitin ligase RNF5 regulates antiviral responses by mediating degradation of the adaptor protein MITA. *Immunity* **30**, 397-407 (2009).
35. Ryan, M.T. & Hoogenraad, N.J. Mitochondrial-nuclear communications. *Annu Rev Biochem* **76**, 701-722 (2007).
36. Rath, E. & Haller, D. Mitochondria at the interface between danger signaling and metabolism: role of unfolded protein responses in chronic inflammation. *Inflammatory bowel diseases* **18**, 1364-1377 (2012).
37. Novak, E.A. & Mollen, K.P. Mitochondrial dysfunction in inflammatory bowel disease. *Front Cell Dev Biol* **3**, 62 (2015).
38. West, A.P., Shadel, G.S. & Ghosh, S. Mitochondria in innate immune responses. *Nature reviews. Immunology* **11**, 389-402 (2011).
39. Szendroedi, J., Phielix, E. & Roden, M. The role of mitochondria in insulin resistance and type 2 diabetes mellitus. *Nature reviews. Endocrinology* **8**, 92-103 (2012).
40. Witte, M.E., Mahad, D.J., Lassmann, H. & van Horssen, J. Mitochondrial dysfunction contributes to neurodegeneration in multiple sclerosis. *Trends in molecular medicine* **20**, 179-187 (2014).
41. Bueno, M.*, et al.* PINK1 deficiency impairs mitochondrial homeostasis and promotes lung fibrosis. *The Journal of clinical investigation* **125**, 521-538 (2015).
42. Nisoli, E., Clementi, E., Carruba, M.O. & Moncada, S. Defective mitochondrial biogenesis: a hallmark of the high cardiovascular risk in the metabolic syndrome? *Circulation research* **100**, 795-806 (2007).
43. Donohoe, D.R.*, et al.* The microbiome and butyrate regulate energy metabolism and autophagy in the mammalian colon. *Cell metabolism* **13**, 517-526 (2011).
44. Bar, F.*, et al.* Mitochondrial gene polymorphisms that protect mice from colitis. *Gastroenterology* **145**, 1055-1063.e1053 (2013).
45. Hooper, L.V.*, et al.* Molecular analysis of commensal host-microbial relationships in the intestine. *Science (New York, N.Y.)* **291**, 881-884 (2001).
46. Santhanam, S.*, et al.* Mitochondrial electron transport chain complex dysfunction in the colonic mucosa in ulcerative colitis. *Inflammatory bowel diseases* **18**, 2158-2168 (2012).
47. Szabo, C. Hydrogen sulphide and its therapeutic potential. *Nature reviews. Drug discovery* **6**, 917-935 (2007).
48. Nagai, T., Abe, A. & Sasakawa, C. Targeting of enteropathogenic Escherichia coli EspF to host mitochondria is essential for bacterial pathogenesis: critical role of the 16th leucine residue in EspF. *The Journal of biological chemistry* **280**, 2998-3011 (2005).
49. Ashktorab, H.*, et al.* Bax translocation and mitochondrial fragmentation induced by Helicobacter pylori. *Gut* **53**, 805-813 (2004).

50. Hernandez, L.D., Pypaert, M., Flavell, R.A. & Galan, J.E. A Salmonella protein causes macrophage cell death by inducing autophagy. *J Cell Biol* **163**, 1123-1131 (2003).
51. Ma, C.*, et al.* Citrobacter rodentium infection causes both mitochondrial dysfunction and intestinal epithelial barrier disruption in vivo: role of mitochondrial associated protein (Map). *Cellular microbiology* **8**, 1669-1686 (2006).
52. Pagliarini, D.J.*, et al.* A mitochondrial protein compendium elucidates complex I disease biology. *Cell* **134**, 112-123 (2008).
53. Paterson, J.K. & Gottesman, M.M. P-Glycoprotein is not present in mitochondrial membranes. *Experimental cell research* **313**, 3100-3105 (2007).
54. Smith, W.W.*, et al.* Kinase activity of mutant LRRK2 mediates neuronal toxicity. *Nature neuroscience* **9**, 1231-1233 (2006).
55. Bonifati, V.*, et al.* Mutations in the DJ-1 gene associated with autosomal recessive early-onset parkinsonism. *Science (New York, N.Y.)* **299**, 256-259 (2003).
56. Langston, J.W., Ballard, P., Tetrud, J.W. & Irwin, I. Chronic Parkinsonism in humans due to a product of meperidine-analog synthesis. *Science (New York, N.Y.)* **219**, 979-980 (1983).
57. Betarbet, R.*, et al.* Chronic systemic pesticide exposure reproduces features of Parkinson's disease. *Nature neuroscience* **3**, 1301-1306 (2000).
58. Panov, A.*, et al.* Rotenone model of Parkinson disease: multiple brain mitochondria dysfunctions after short term systemic rotenone intoxication. *The Journal of biological chemistry* **280**, 42026-42035 (2005).
59. Franke, A.*, et al.* Genome-wide meta-analysis increases to 71 the number of confirmed Crohn's disease susceptibility loci. *Nature genetics* **42**, 1118-1125 (2010).
60. Cadwell, K.*, et al.* Virus-plus-susceptibility gene interaction determines Crohn's disease gene Atg16L1 phenotypes in intestine. *Cell* **141**, 1135-1145 (2010).
61. Yan, H., Wang, H., Zhang, X., Li, X. & Yu, J. Ascorbic acid ameliorates oxidative stress and inflammation in dextran sulfate sodium-induced ulcerative colitis in mice. *Int J Clin Exp Med* **8**, 20245-20253 (2015).
62. Bulua, A.C.*, et al.* Mitochondrial reactive oxygen species promote production of proinflammatory cytokines and are elevated in TNFR1-associated periodic syndrome (TRAPS). *The Journal of experimental medicine* **208**, 519-533 (2011).
63. Zhou, R., Yazdi, A.S., Menu, P. & Tschopp, J. A role for mitochondria in NLRP3 inflammasome activation. *Nature* **469**, 221-225 (2011).
64. Nakahira, K.*, et al.* Autophagy proteins regulate innate immune responses by inhibiting the release of mitochondrial DNA mediated by the NALP3 inflammasome. *Nature immunology* **12**, 222-230 (2011).
65. Zhang, Q.*, et al.* Circulating mitochondrial DAMPs cause inflammatory responses to injury. *Nature* **464**, 104-107 (2010).
66. Oka, T.*, et al.* Mitochondrial DNA that escapes from autophagy causes inflammation and heart failure. *Nature* **485**, 251-255 (2012).
67. Tal, M.C.*, et al.* Absence of autophagy results in reactive oxygen species-dependent amplification of RLR signaling. *Proceedings of the National Academy of Sciences of the United States of America* **106**, 2770-2775 (2009).
68. Saitoh, T.*, et al.* Loss of the autophagy protein Atg16L1 enhances endotoxin-induced IL-1beta production. *Nature* **456**, 264-268 (2008).

Figures

Figure 1. Damaged mitochondria accumulate within *mdr1a*-deficient colonic epithelium: (a) Representative TEM (n=6 per group) of colonic epithelium. Scale bar 2μm. Yellow arrows denoting damaged mitochondria. (b) Quantitative analyses of CEC containing damaged mitochondria (n=6/group). (c) Representative H&E and immunohistochemistry of colon (p62, PINK-1, SOD2 and VDAC) (n=6/group). (d) Loss of mitochondria membrane potential, JC-1 fluorescence in isolated mitochondria (n=6/group) (e) Plasma qPCR of mitochondrial DNA *mdr1a*$^{-/-}$ mice with colitis vs. no colitis (n=8/group). WT – wild-type. All data represent mean± SEM.

Figure 2. MDR1 deficiency results in mitochondria dysfunction: (a) Oxygen consumption rate, OCR (pmol/minute) in primary colonic explant in *mdr1a*-deficient vs. WT respectively (n=4). (b) Spare respiratory capacity (SRC) of T84 *shMDRI* and *shCtrl* (5 replicates). (c) Normalised MitoSOX/Mitotracker Green fluorescence T84 *shMDR1* vs. *shCtrl*, (n=11/group, representative of 3 independent experiments. (d) Relative MitoSOX/Mitotracker Green fluorescence to respective untreated group in T84 *shMDR1* vs. *shCtrl* (n=8/treatment group, representative of 3 independent experiments). (e) Quantification of GFP-LC3 *shMDR1* vs. *shCtrl* (n=12 slides/group). %GFP-LC3+ve cells/number of cells in 10 fields (X40 microscopy). All data represent mean± SEM.

Figure 3. Experimental induction of mROS accelerates spontaneous colitis in *mdr1a*-deficiency and in acute DSS-colitis: (a) Experimental protocol of 4-week colonic administration of rotenone vs. vehicle (3x/week). (b) Prevalence of clinical

colitis in rotenone vs. vehicle treated *mdr1a*$^{-/-}$ at weekly intervals (n=18 and 15 mice treated with rotenone and vehicle respectively). (c) Stool consistency measurements in rotenone vs. vehicle treated *mdr1a*$^{-/-}$ at weekly intervals. (d) Representative images of *mdr1a*$^{-/-}$ and WT whole colons treated with colonic rotenone. (e) Histology scores of rotenone vs. vehicle treated *mdr1a*$^{-/-}$ colons. (f) Representative H&E distal and proximal colons; and histology scores of rotenone vs. vehicle treated *mdr1a*$^{-/-}$, black scale bars 100 μm. (g) Experimental protocol of colonic rotenone vs. vehicle – 3 times during 7-day 2% DSS in drinking water. (h) Daily percentage of change from initial weight in rotenone vs. vehicle treated *mdr1a*$^{-/-}$ acute DSS colitis (n=7/group). (i, j) Representative histology scores and H&E colons of rotenone vs. vehicle treated *mdr1a*$^{-/-}$ (n=7/group) in acute DSS colitis, black scale bar 50μm. All data represent mean± SEM.

Figure 4. Inhibition of mitochondria ROS effects attenuates and promotes recovery from colitis: (a) Experimental protocol of 4-week colonic administration of rotenone vs. vehicle vs. MQ (3x/week) in *mdr1a*$^{-/-}$ with established chronic colitis. (b) Stool consistency measurements in rotenone vs. vehicle treated vs. MQ in *mdr1a*$^{-/-}$ at weekly intervals. (c) Histology colitis scores of rotenone vs. vehicle vs. MQ vs. non-colitic *mdr1a*$^{-/-}$ mice. (d) Representative whole colons and spleen sizes of and H&E of rotenone vs. vehicle vs. MQ vs. non-colitic *mdr1a*$^{-/-}$ mice. (e) Experimental protocol of colonic MQ vs. vehicle – 3x administrations during 7-day 2% DSS colitis protocol. (f, g) Daily percentages change from initial weight clinical colitis in MQ vs. vehicle in *mdr1a*$^{-/-}$ (n=6/group) and and WT mice (n=6/group) respectively. (h) Histology colitis scores in MQ vs. vehicle treated *mdr1a*$^{-/-}$ and WT mice, scale bar 50μm. (i) Experimental protocol of colonic MQ vs. vehicle treatment after 5 days of 2% DSS

colitis protocol in WT mice. (j) Daily percentages of change from initial weight in MQ vs. vehicle treated WT, (n=8/7 respectively). All data represent mean± SEM.

Figure 5. *MDR1* and *SOD2* genes are differentially expressed in human IBD and intestinal epithelial specific deletion of *SOD2* leads to increased susceptibility to experimental colitis: (a-b) *In silico* analysis of *MDR1* and *SOD2* from 120 IBD patients (67 UC, 53 CD, 17 non-IBD colitis and 31 healthy controls); IBD-Inf = Inflamed IBD gut biopsies, IBD-Non-Inf = Non-inflamed IBD gut biopsies; Control-Inf = Non-IBD colitis and Control-Non-Infl =Non-inflamed gut biopsies from non-IBD individuals. (c) Spearman's correlation test of *MDR1* and *SOD2* expression in 120 IBD patients. (d) Representative immunohistochemistry and Western blotting of SOD2 of colons (a) of $SOD2^{IEC\text{-}KO}$ and $SOD2^{flox/flox}$ of CECs, black scale bars 100 μm, yellow arrows showing SOD2 staining. (e) Daily percentages of weight change from initial weight in acute 2% DSS colitis comparing $SOD2^{IEC\text{-}KO}$ vs. $SOD2^{flox/flox}$ (n=12/8 respectively). (f) Histology colitis scores in $SOD2^{IEC\text{-}KO}$ vs. $SOD2^{flox/flox}$ mice (n=12/8 respectively) after 2% DSS colitis. (g) Representative H&E staining in $SOD2^{IEC\text{-}KO}$ vs. $SOD2^{flox/flox}$ mice after 2% DSS colitis, black scale bars 100 μm. All data represent mean± SEM.

Supplementary Figures Information

S1. (a) Representative TEM sections of liver, ileum and lung from $mdr1a^{-/-}$ and WT mice (n=6) Scale bar 2μm. (b) TEM sections of colons from $il10^{-/-}$ and WT-following 3 days of 3% DSS colitis. Orange scale bar is 2μm and white scale bar is 0.5μm. Yellow asterisks – denoting abnormal mitochondria.

S2. (a) Western blot analyses of p62, Parkin, PINK, LC3I-II in isolated mouse CECs (n=3/group). (b) Quantitative PCR of mitochondria DNA normalised to nuclear *18S* in CECs (n=6/group). (c) Immunohistochemistry of Ki67 in colon sections (n=6/group). Quantification in right panel, black scale bar 100μm (d) TUNEL assay (green: quantification in right panel), white scale bar 100μm (n=6/group). WT – wild-type. All data represent mean± SEM.

S3. (a) (b) Quantitative PCR of *MDR1* gene (triplicate) and representative Western blotting of MDR1 (C219) in T84 *shMDRI* and *shCtrl*. (c) Basal OCR of T84 *shMDRI* and *shCtrl* (5 replicates). (d) Western blotting of p62 and SOD2 and, (e) LC3I/II in untreated or bafilomycin (100nM for 2 hours) treated *shMDR1* vs. *shCtrl* CECs (representative of 2 independent experiments). All data represent mean± SEM.

S4. (a) Representative H&E colon sections following colonic treatment with rotenone at 1, 10 and 100μM (3x/week and harvested at Day 7; n=4/group) in WT mice. (b) Representative H&E colon sections and (c) histology colitis scores of *mdr1a*$^{-/-}$ and WT mice (n=5 in 0.25% DSS groups and n=6 in rotenone groups), black scale bar 100μm, yellow arrows indicating leukocyte infiltration. (d) Representative TUNEL staining in *mdr1a*$^{-/-}$ and WT mice (n=3/group) and (e) quantification of TUNEL+ve CECs (green: quantification in right panel), white scale bar 100μm. (e) qPCR analyses of isolated CECs in rotenone vs. vehicle treated *mdr1a*$^{-/-}$ and untreated WT mice (n=6/group). *$p<0.05$ comparing vehicle vs. rotenone treatment in *mdr1a*$^{-/-}$ mice. All data represent mean± SEM.

S5. (a) Western blotting of PARP and cleaved PARP products in T84 *shMDR1* vs. *shCtrl* treated with rotenone (10μM), CCCP (10μM), Cisplatin 10ng/ml for 12 hours in T84 *shMDR1* vs. *shCtrl*. (b) Live cell imaging of T84 *shMDR1* vs. *shCtrl* treated with rotenone (5μM) at 0 and 24 hours. Loss of viability – rounded appearance, increased lucency and decreased adherence. (c) Rate of transepithelial electrical resistance (TEER) loss in T84 *shMDR1* vs. *shCtrl* grown on 12-well transwell plates following culture with rotenone 5μM, (n=3). (d) IL-8 ELISA of T84 *shMDR1* vs. *shCtrl* 12 hours following co-culture with rotenone (10μM), flagellin (10ng/ml) and bacterial CpG (2μM) (n=2/treatment group, representative of 2 independent experiments), R=rotenone, F=flagellin. All data represent mean± SEM.

S6. (a) Representative H&E staining of rotenone vs. vehicle vs. MQ vs. non-colitic *mdr1a*$^{-/-}$ colons. (b) Representative H&E staining of MQ vs. vehicle following 7-day 2% DSS colitis protocol in WT and *mdr1a*$^{-/-}$ colons, (c) Representative H&E staining of MQ vs. vehicle treated WT colons following 5-day 2% DSS and 5-days recovery, scale bar 50μm.

Supplementary Material and Methods

Immunohistochemistry, Western blotting and qPCR

Formalin-fixed paraffin-embedded sections were stained according to standard immunohistochemistry protocols and Ab dilutions are available on request. Cell death was assessed by TdT-mediated dUTP nick end labelling (TUNEL) of formalin-fixed paraffin-embedded slides using *in situ* TUNEL cell death detection kit (Roche). We enumerated total TUNEL^{+} and Ki67^{+} IECs in entire colonic slide sections and data

expressed as percentage of total IECs (>3 slides per subject). For Western blotting, cells were lysed with RIPA buffer, protein quantification by Bradford protocol, 20-40 µg of total protein was applied to each lane and subjected to SDS-PAGE and Western blotting via enhanced chemiluminescence (Luminata Classico, Millipore). Total RNA was isolated from cells using RNeasy Mini kit (QIAGEN) and qPCR performed with SYBR Green RT-PCR Kit (Qiagen Cat # 204243) on ABI 7900 system. Experimental groups were compared using ΔΔCt values. Mouse *KC* 5-GGCTGGGATTCACCTCAAGAA-3, 5-CTTGGGGACACCTTTTAGCATC-3; *il-6* 5-GATGGATGCTACCAAACTGGA-3, 5-GGAAATTGGGGTAGGAAGGA-3; *tnf-α* 5-CTGGGACAGTGACCTGGACT-3, 5-GCACCTCAGGGAAGAGTCTG-3; mouse *18S* Housekeeping FORWARD, 5-TAGAGGGACAAGTGGCGTTC-3; REVERSE 5-CGCTGAGCCAGTCAGTGT-3.

Chemicals

Anti-p62/SQSTM1 (1:1000 IHC, MBL), monoclonal anti-SOD2 (ab68155), polyclonal anti-SOD2 (1:50, PA5-30604 Thermoscientific), anti-VDAC (Abcam ab18988), PARP (Cell signalling), anti-PINK-1 (1:100 IHC, Abcam ab23707), anti-Parkin (Abcam ab81153), anti-Ki67 (Novo castra NCL-Ki67p), anti-TLR9 (abcam ab52967). Antimycin A (A8674-Sigma), Rotenone (R8875-Sigma), Carbonyl-cyanide 4-(trifluoromethoxy) phenylhydrazone, CCCP (C2920 – Sigma), Bafilomycin (B1793-Sigma) TLR9 antagonist ODN TTAGGG (Invivogen), Lipofectamine (ThermoFisher). $MitoQ_{10}$ was a kind gift from Dr Mike Murphy, University of Cambridge. Mitotracker Green and MitoSOX (Molecular Probes). GFP-LC3 plasmid was kindly provided by Dr C Stevens, University of Edinburgh. IL-8 and IL-6 ELISA (Cambridge Bioscience).

Mouse genotyping primers

SOD2: LoxNeo 5-AGCTTGGCTGGACGTAA-3, *MnSOD#42* 5-CGAGGGGCATCT AGTGGAGAA-3; *P2* 5-TTAGGGCTCAGGTTTGTCCAGAA-3; Flox-allele 358 bp, wild-type 500 bp; 95C for 5 mins, 32 cycles of 94C for 1 min, 58C for 1 min, 72C for 2 mins and finally 72C for 10 mins. IMR 1878 5-GTGTGGGACAGAGAACAAACC-3, IMR 1879 5-ACATCTTCAGGTTCTGCGGG-3; 94C for 3 mins, 35 cycles of 94C for 30 seconds, 64C for 1 min, 72C for 1.5 min and finally 72C for 2 mins; villin-Cre transgene 1100 bp.

Table S6: Genes involved in mitochondria function (using gene-set defined by term GO:0005739) within subset of 574 genes within 100 kb of loci with genome wide statistical significant association with inflammatory bowel disease ($p<5 \times 10^{-8}$).

Gene	Gene ID	P-value	Protein Name
SLC25A28	81894	1.70×10^{-26}	Mitoferrin-2
VARS	7407	4.83×10^{-26}	Valine--tRNA ligase
RNF5	6048	9.47×10^{-24}	E3 ubiquitin-protein ligase RNF5
HSPA1A	3303	1.88×10^{-23}	Heat shock 70 kDa protein 1A/1B
HSPA1B	3304	1.88×10^{-23}	Heat shock 70 kDa protein 1A/1B
HSPA1L	3305	1.88×10^{-23}	Heat shock 70 kDa protein 1-like
TAP1	6890	2.78×10^{-21}	Antigen peptide transporter 1
GPX1	2876	2.40×10^{-20}	Glutathione peroxidase 1
SLC22A4	6583	7.07×10^{-17}	Solute carrier family 22 member 4
PLA2G2A	5320	2.31×10^{-16}	Phospholipase A2, membrane associated
MCCD1	401250	4.56×10^{-16}	Mitochondrial coiled-coil domain protein 1
STARD3	10948	1.35×10^{-15}	StAR-related lipid transfer protein 3
LRRK2	120892	3.18×10^{-15}	Leucine-rich repeat serine/threonine-protein kinase 2
DLD	1738	4.50×10^{-14}	Dihydrolipoyl dehydrogenase, mitochondrial
STAT3	6774	2.16×10^{-12}	Signal transducer and activator of transcription
PTRF	284119	2.16×10^{-12}	Polymerase I and transcript release factor
GPX4	2879	2.37×10^{-11}	Phospholipid hydroperoxide glutathione peroxidase, mitochondrial
TUFM	7284	3.86×10^{-10}	Elongation factor Tu, mitochondrial
PARK7	11315	7.36×10^{-10}	Protein DJ-1
NDUFAF3	25915	7.92×10^{-10}	NADH dehydrogenase [ubiquinone]1 alpha subcomplex assembly factor 3
SLC25A20	788	1.06×10^{-9}	Mitochondrial carnitine/acylcarnitine carrier protein
ATG5	9474	1.26×10^{-9}	Autophagy protein 5
TRIM39	56658	1.46×10^{-9}	E3 ubiquitin-protein ligase TRIM39
C6orf136	221545	2.77×10^{-9}	Uncharacterized protein C6orf136
TRIM31	11074	1.02×10^{-8}	E3 ubiquitin-protein ligase TRIM31
SDHC	6391	1.08×10^{-8}	Succinate dehydrogenase cytochrome b560 subunit, mitochondrial
UQCR10	29796	4.54×10^{-8}	Cytochrome b-c1 complex subunit 9
VARS2	57176	1.21×10^{-9}	Valine--tRNA ligase, mitochondrial

Fig 1

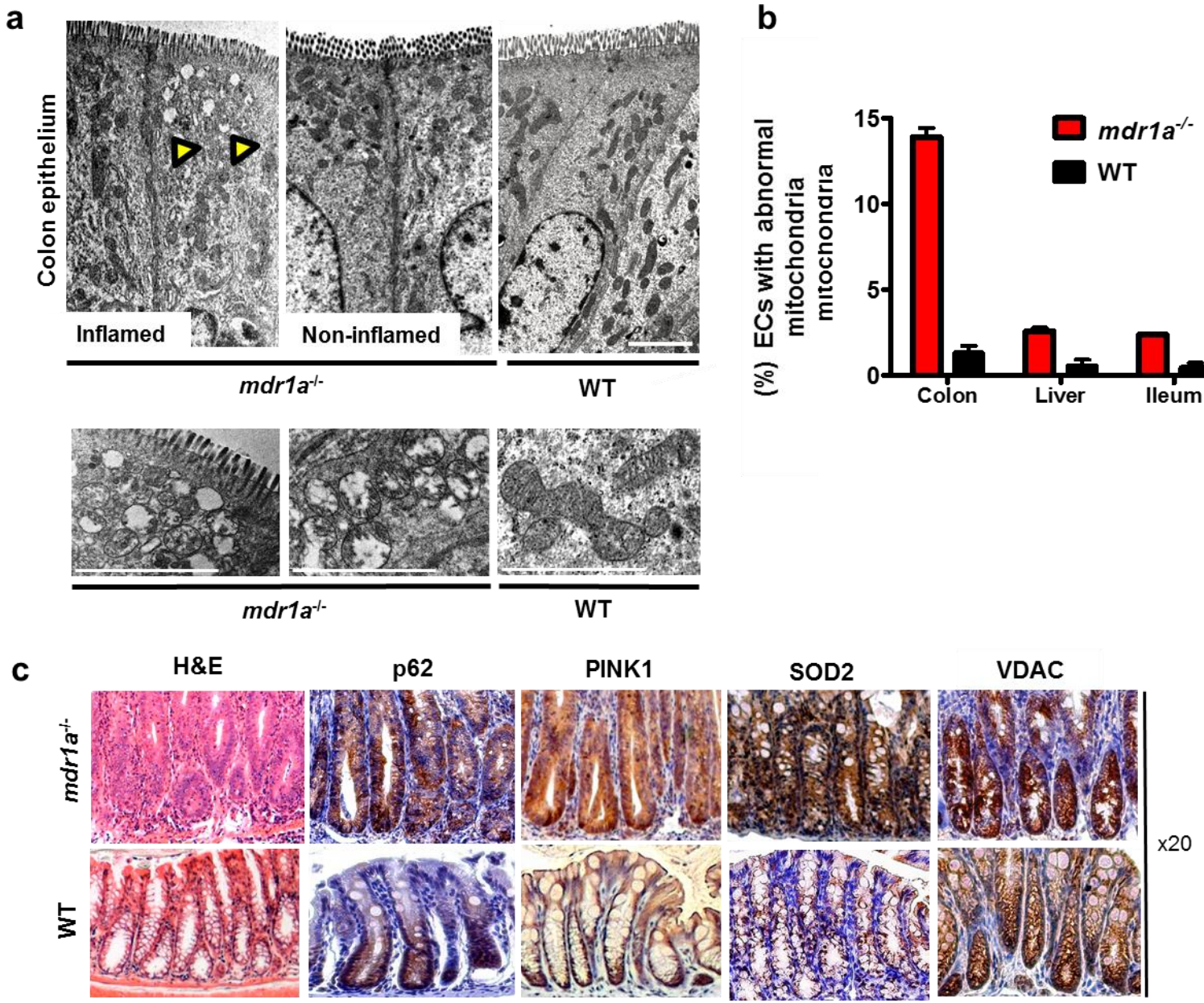
a
Colon epithelium
Inflamed
Non-inflamed
mdr1a-/-
WT
mdr1a-/-
WT
b
(%) ECs with abnormal mitochondria
15
10
5
0
mdr1a-/-
WT
Colon
Liver
Ileum
d
mdr1a-/-
WT
ΔΨ Mitochondria (%)
100
50
0
p<0.001
Control
+CCCP
c
H&E
p62
PINK1
SOD2
VDAC
mdr1a-/-
WT
x20
e
Mitochondria DNA (copies/ml)
6000
4000
2000
0
p=0.005
Colitis
No Colitis

Fig 2

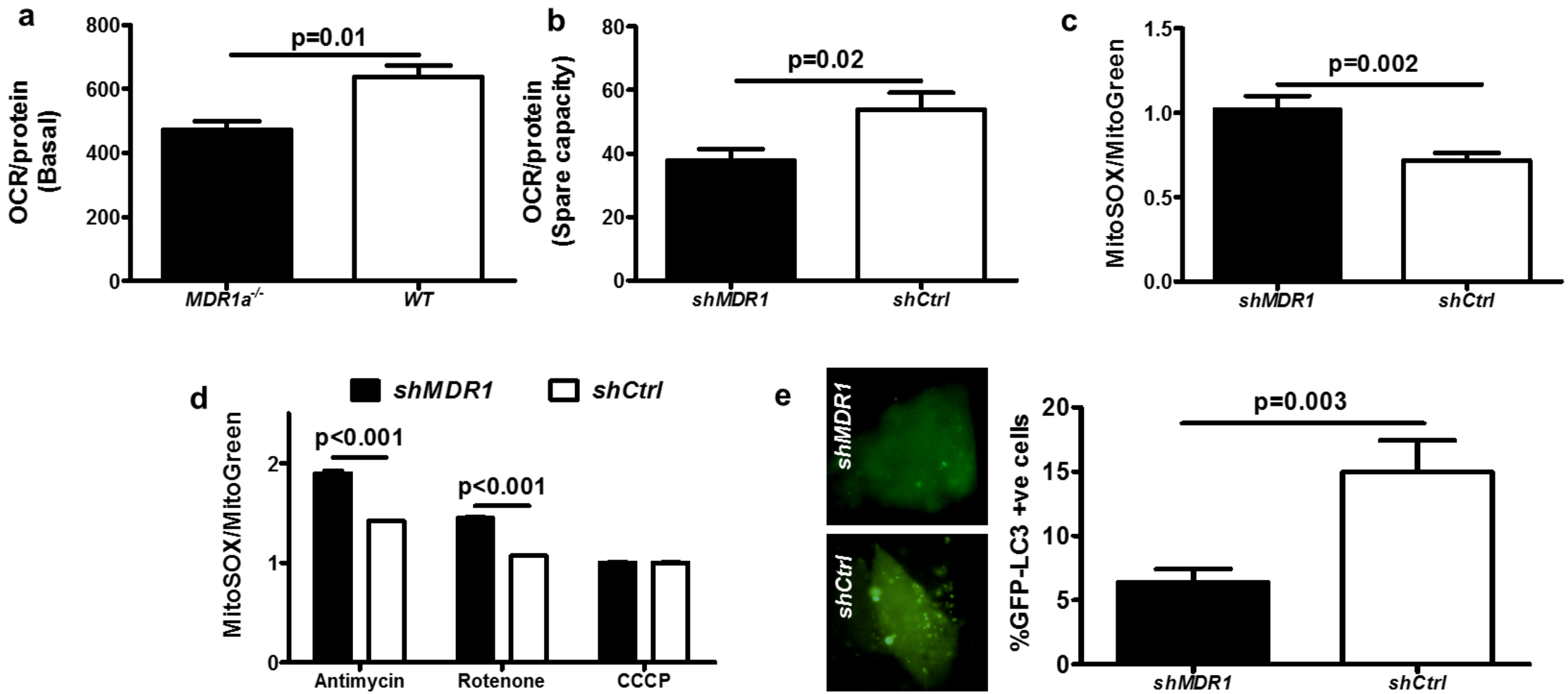
a
OCR/protein (Basal)
800
600
400
200
0
p=0.01
MDR1a-/-
WT
b
OCR/protein (Spare capacity)
80
60
40
20
0
p=0.02
shMDR1
shCtrl
c
MitoSOX/MitoGreen
1.5
1.0
0.5
0.0
p=0.002
shMDR1
shCtrl
d
shMDR1
shCtrl
MitoSOX/MitoGreen
2
1
0
p<0.001
p<0.001
Antimycin
Rotenone
CCCP
e
shMDR1
shCtrl
%GFP-LC3 +ve cells
20
15
10
5
0
p=0.003
shMDR1
shCtrl

Fig 3

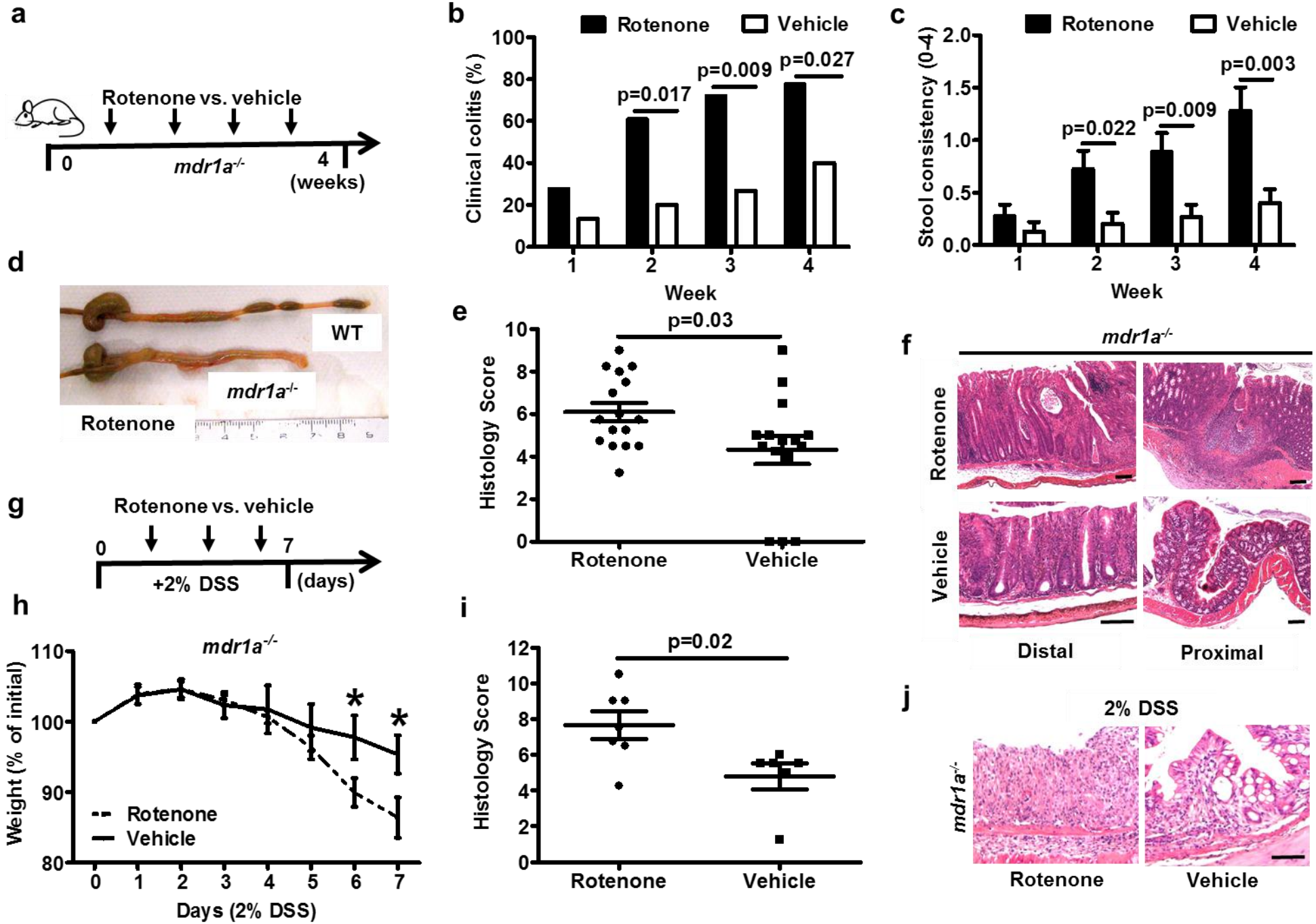
a
Rotenone vs. vehicle
0
mdr1a-/-
4
(weeks)
b
Rotenone
Vehicle
Clinical colitis (%)
p=0.017
p=0.009
p=0.027
Week
c
Rotenone
Vehicle
Stool consistency (0-4)
p=0.022
p=0.009
p=0.003
Week
d
WT
mdr1a-/-
Rotenone
e
Histology Score
p=0.03
Rotenone
Vehicle
f
mdr1a-/-
Rotenone
Vehicle
Distal
Proximal
g
Rotenone vs. vehicle
0
7
+2% DSS
(days)
h
mdr1a-/-
Weight (% of initial)
Rotenone
Vehicle
Days (2% DSS)
i
Histology Score
p=0.02
Rotenone
Vehicle
j
2% DSS
mdr1a-/-
Rotenone
Vehicle

Fig 4

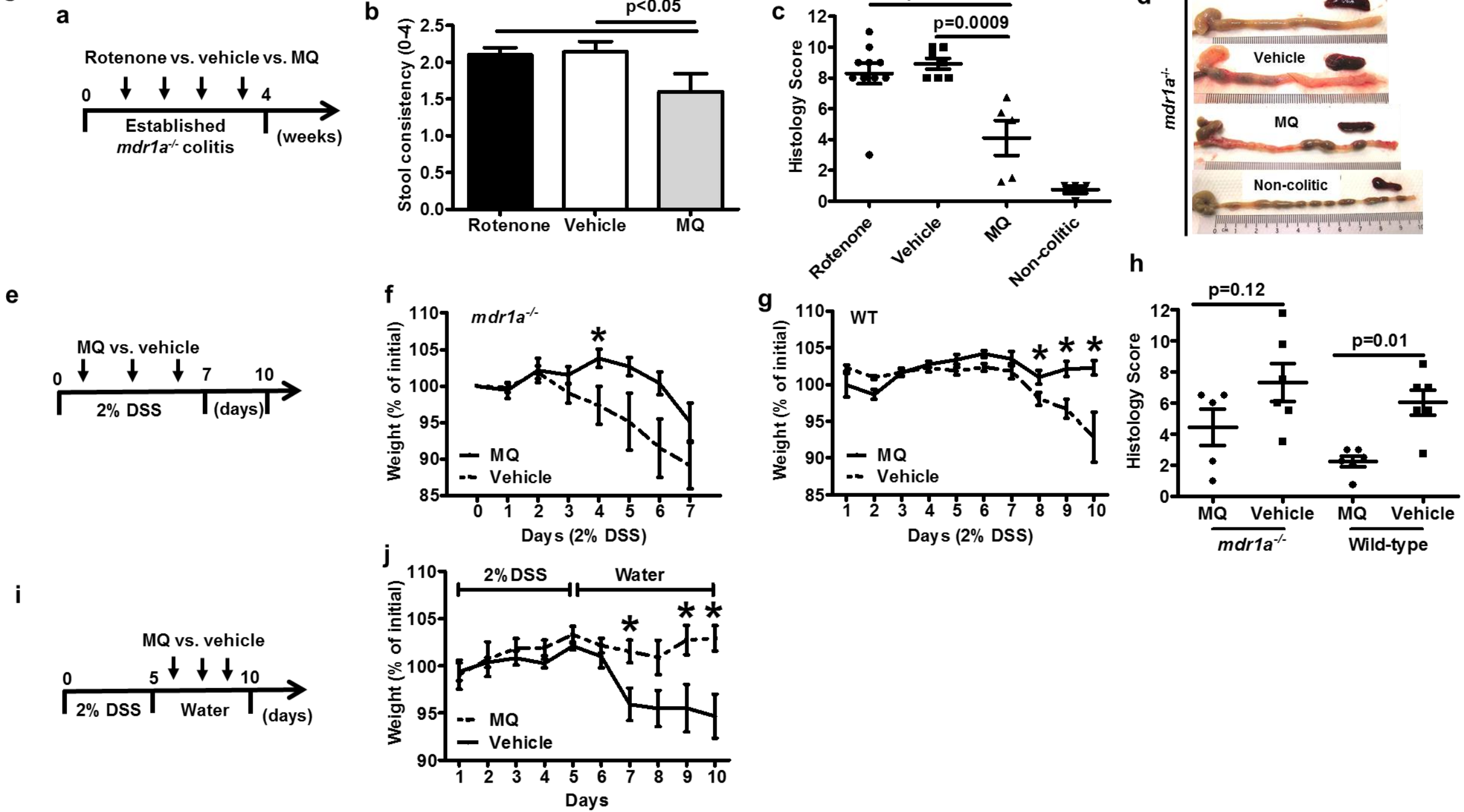
a
Rotenone vs. vehicle vs. MQ
0
4
Established
mdr1a-/- colitis
(weeks)
b
p<0.05
Stool consistency (0-4)
2.5
2.0
1.5
1.0
0.5
0.0
Rotenone
Vehicle
MQ
c
p=0.005
p=0.0009
Histology Score
12
10
8
6
4
2
0
Rotenone
Vehicle
MQ
Non-colitic
d
mdr1a-/-
Rotenone
Vehicle
MQ
Non-colitic
e
MQ vs. vehicle
0
7
10
2% DSS
(days)
f
mdr1a-/-
Weight (% of initial)
110
105
100
95
90
85
MQ
Vehicle
0 1 2 3 4 5 6 7
Days (2% DSS)
g
WT
Weight (% of initial)
110
105
100
95
90
85
MQ
Vehicle
1 2 3 4 5 6 7 8 9 10
Days (2% DSS)
h
p=0.12
p=0.01
Histology Score
12
10
8
6
4
2
0
MQ
Vehicle
MQ
Vehicle
mdr1a-/-
Wild-type
i
MQ vs. vehicle
0
5
10
2% DSS
Water
(days)
j
2% DSS
Water
Weight (% of initial)
110
105
100
95
90
MQ
Vehicle
1 2 3 4 5 6 7 8 9 10
Days

Fig 5

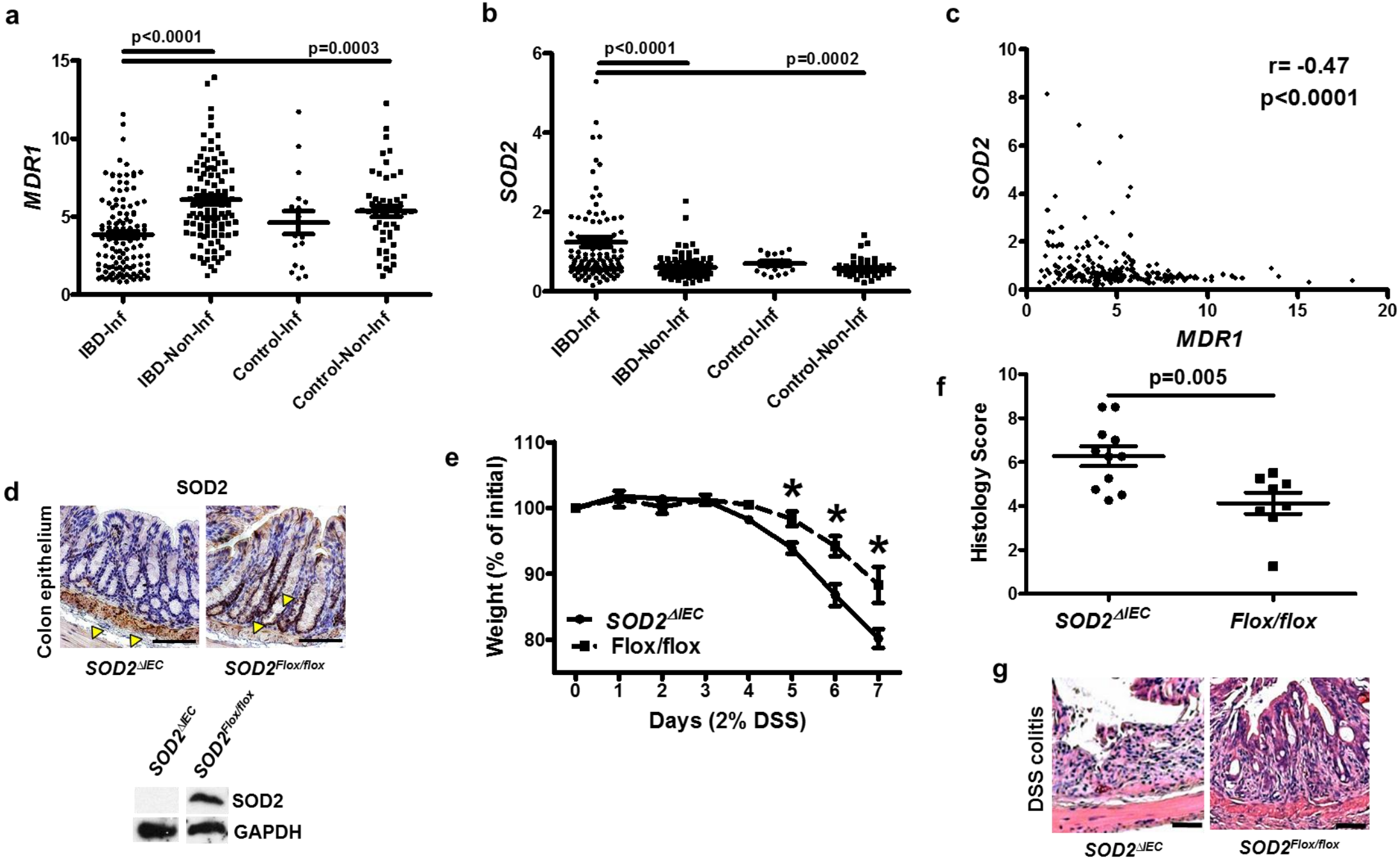
a
p<0.0001
p=0.0003
MDR1
IBD-Inf
IBD-Non-Inf
Control-Inf
Control-Non-Inf
b
p<0.0001
p=0.0002
SOD2
c
r= -0.47
p<0.0001
SOD2
MDR1
d
SOD2
Colon epithelium
SOD2ΔIEC
SOD2Flox/flox
GAPDH
e
Weight (% of initial)
Days (2% DSS)
f
p=0.005
Histology Score
g
DSS colitis

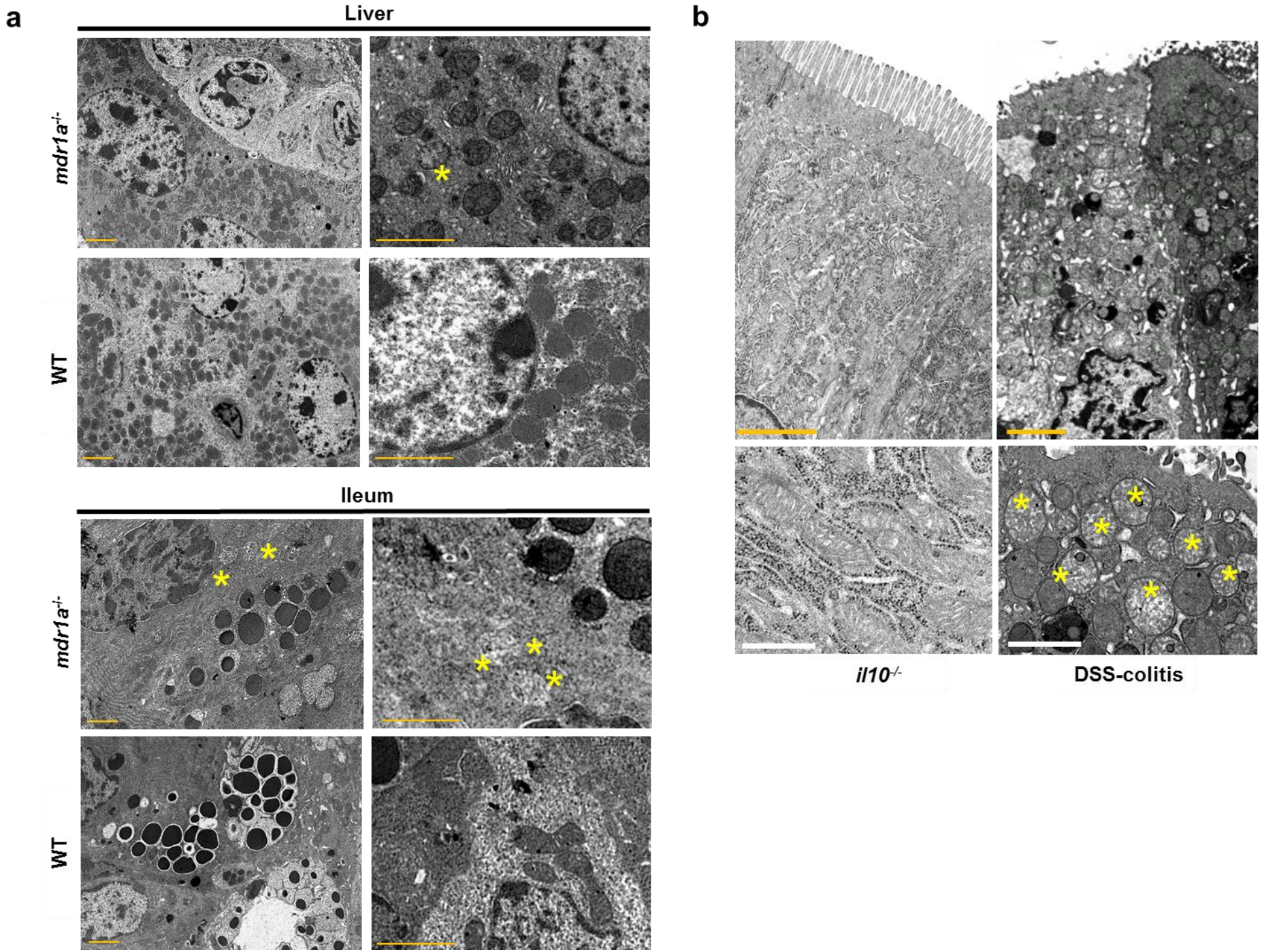
a
Liver
mdr1a-/-
WT
Ileum
mdr1a-/-
WT
b
il10-/-
DSS-colitis

SI 2

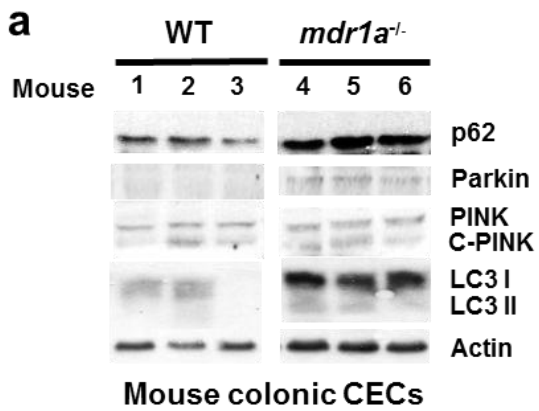
a
WT
mdr1a-/-
Mouse
1 2 3 4 5 6
p62
Parkin
PINK
C-PINK
LC3 I
LC3 II
Actin
Mouse colonic CECs

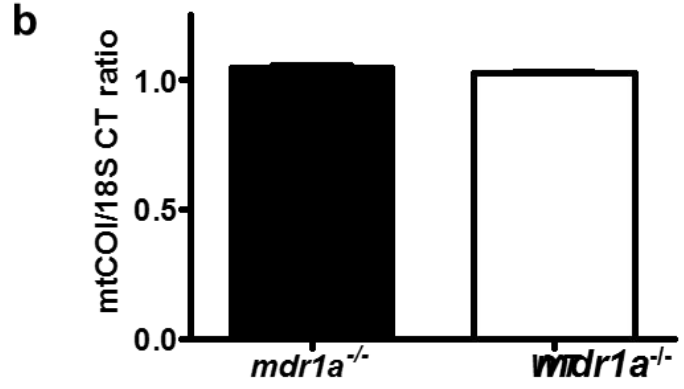
b
mtCOI/18S CT ratio
1.0
0.5
0.0
mdr1a-/-
wtdr1a-/-

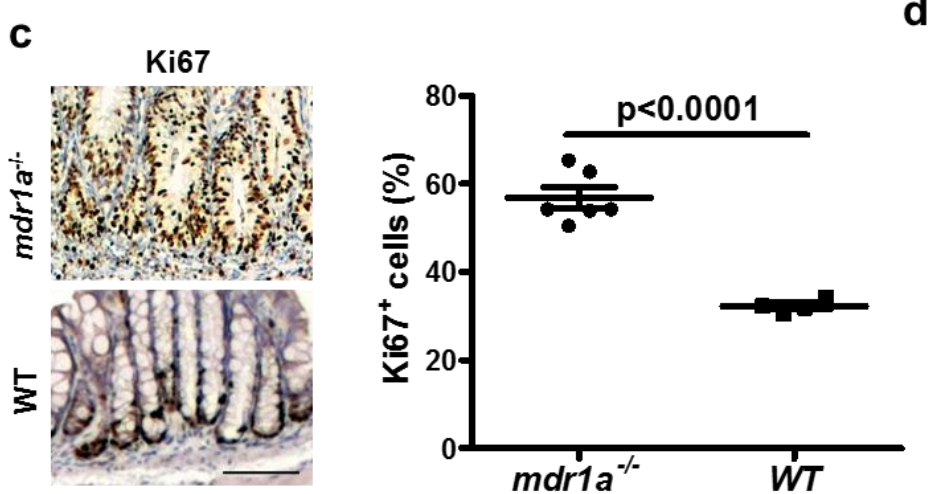
c
Ki67
mdr1a-/-
WT
Ki67+ cells (%)
80
60
40
20
0
p<0.0001
mdr1a-/-
WT

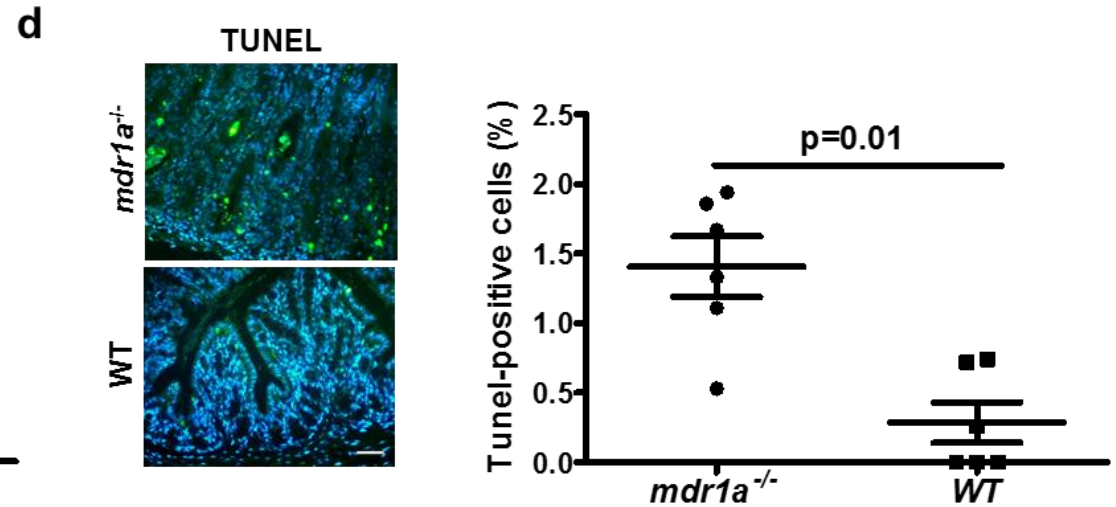
d
TUNEL
mdr1a-/-
WT
Tunel-positive cells (%)
2.5
2.0
1.5
1.0
0.5
0.0
p=0.01
mdr1a-/-
WT

SI 3

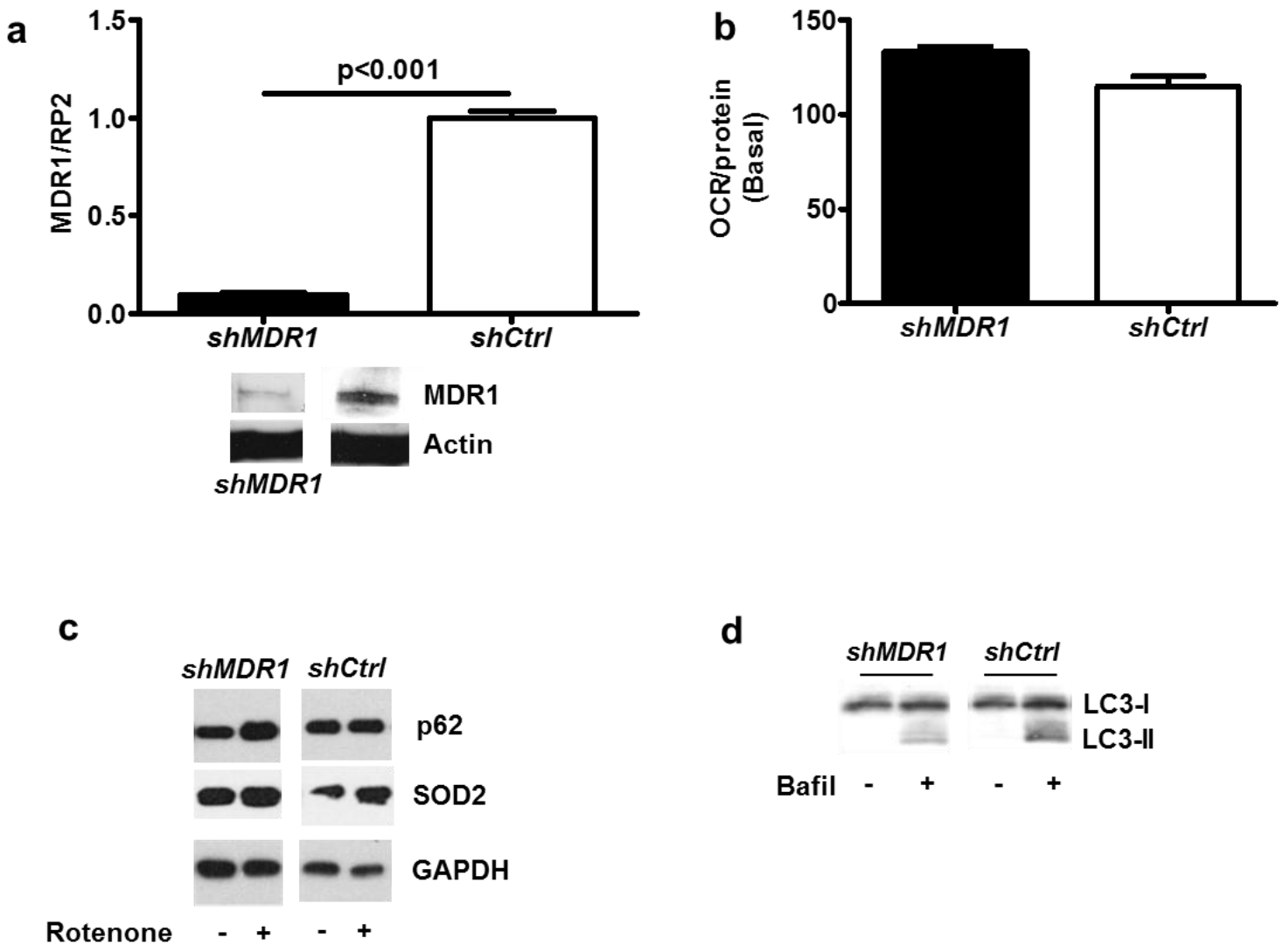
a
1.5
1.0
0.5
0.0
MDR1/RP2
p<0.001
shMDR1
shCtrl
MDR1
Actin
shMDR1
b
150
100
50
0
OCR/protein (Basal)
shMDR1
shCtrl
c
shMDR1
shCtrl
p62
SOD2
GAPDH
Rotenone - + - +
d
shMDR1
shCtrl
LC3-I
LC3-II
Bafil - + - +

SI 4

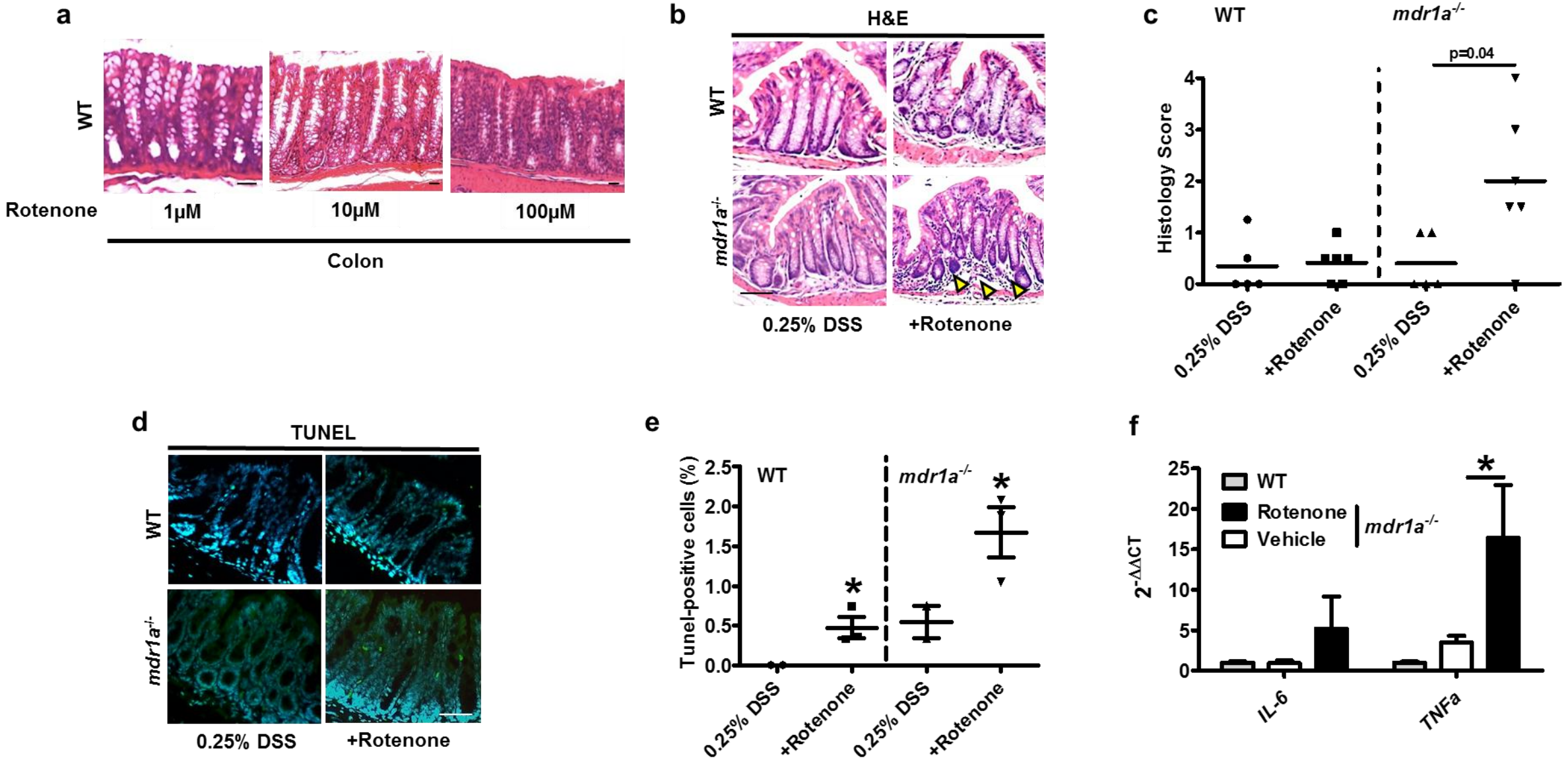
a
WT
Rotenone
1μM
10μM
100μM
Colon
b
H&E
WT
mdr1a-/-
0.25% DSS
+Rotenone
c
WT
mdr1a-/-
p=0.04
Histology Score
0
1
2
3
4
0.25% DSS
+Rotenone
0.25% DSS
+Rotenone
d
TUNEL
WT
mdr1a-/-
0.25% DSS
+Rotenone
e
Tunel-positive cells (%)
0.0
0.5
1.0
1.5
2.0
2.5
WT
mdr1a-/-
*
*
0.25% DSS
+Rotenone
0.25% DSS
+Rotenone
f
2-ΔΔCT
0
5
10
15
20
25
WT
Rotenone
Vehicle
mdr1a-/-
*
IL-6
TNFa

SI 5

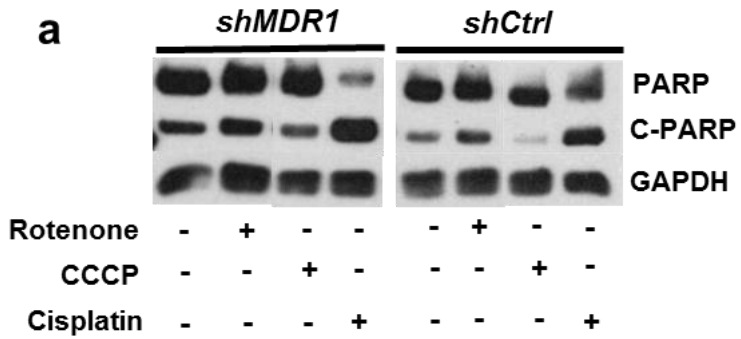
a
shMDR1
shCtrl
PARP
C-PARP
GAPDH
Rotenone - + - - - + - -
CCCP - - + - - - + -
Cisplatin - - - + - - - +

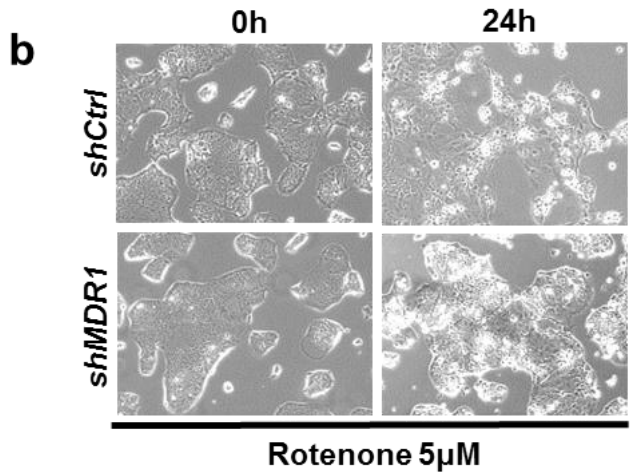
b
0h
24h
shCtrl
shMDR1
Rotenone 5μM

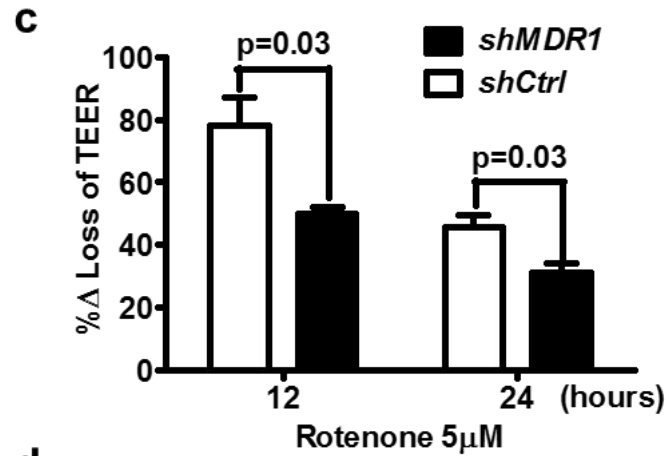
c
p=0.03
p=0.03
shMDR1
shCtrl
%Δ Loss of TEER
100
80
60
40
20
0
12
24 (hours)
Rotenone 5μM

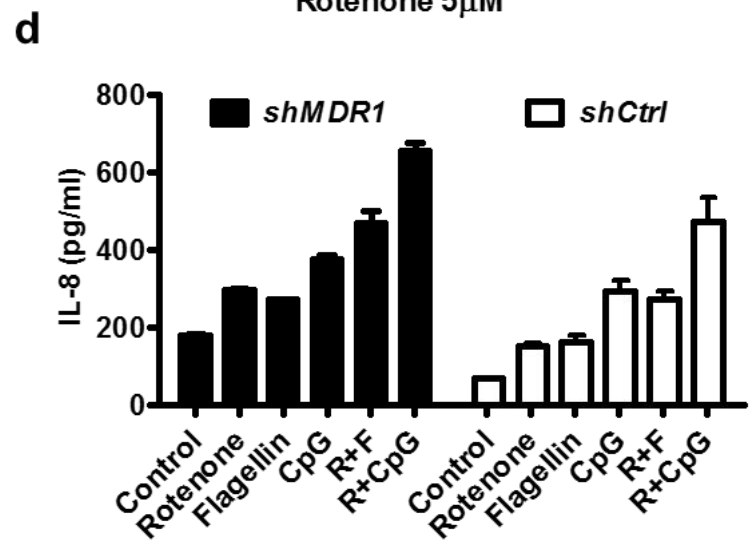
d
shMDR1
shCtrl
IL-8 (pg/ml)
800
600
400
200
0
Control
Rotenone
Flagellin
CpG
R+F
R+CpG
Control
Rotenone
Flagellin
CpG
R+F
R+CpG

SI 6

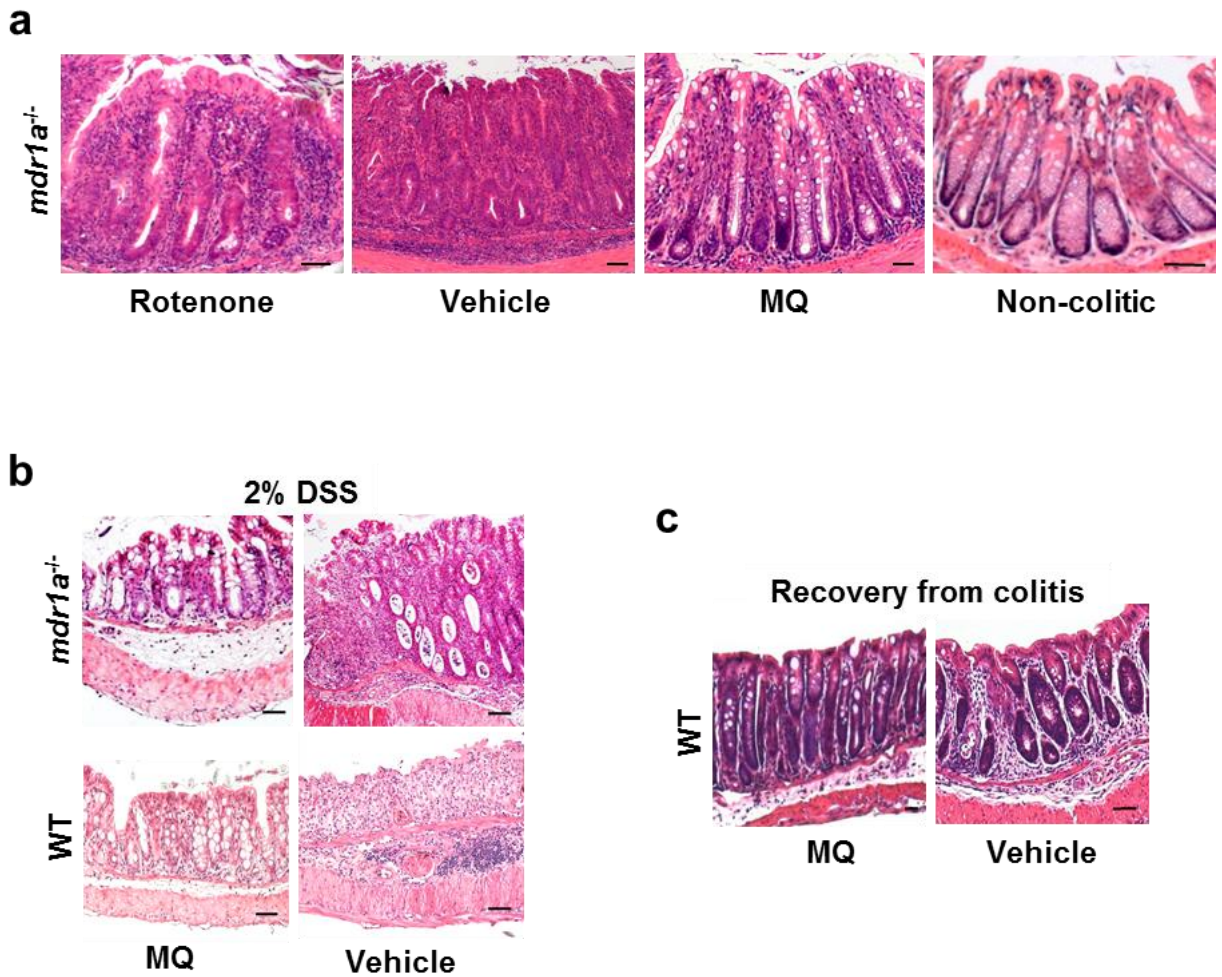
a
mdr1a-/-
Rotenone
Vehicle
MQ
Non-colitic
b
2% DSS
mdr1a-/-
WT
MQ
Vehicle
c
Recovery from colitis
WT
MQ
Vehicle